

---

[All ETDs from UAB](#)

[UAB Theses & Dissertations](#)

---

1987

## **Best Approximate Impulse Response Estimate In Pseudo-Random Binary Sequence System Identification With Application To Sodium Nitroprusside Pharmacodynamics.**

James Ralph Jacobs  
*University of Alabama at Birmingham*

Follow this and additional works at: <https://digitalcommons.library.uab.edu/etd-collection>

---

### **Recommended Citation**

Jacobs, James Ralph, "Best Approximate Impulse Response Estimate In Pseudo-Random Binary Sequence System Identification With Application To Sodium Nitroprusside Pharmacodynamics." (1987). *All ETDs from UAB*. 4312.  
<https://digitalcommons.library.uab.edu/etd-collection/4312>

This content has been accepted for inclusion by an authorized administrator of the UAB Digital Commons, and is provided as a free open access item. All inquiries regarding this item or the UAB Digital Commons should be directed to the [UAB Libraries Office of Scholarly Communication](#).

## **INFORMATION TO USERS**

While the most advanced technology has been used to photograph and reproduce this manuscript, the quality of the reproduction is heavily dependent upon the quality of the material submitted. For example:

- Manuscript pages may have indistinct print. In such cases, the best available copy has been filmed.
- Manuscripts may not always be complete. In such cases, a note will indicate that it is not possible to obtain missing pages.
- Copyrighted material may have been removed from the manuscript. In such cases, a note will indicate the deletion.

Oversize materials (e.g., maps, drawings, and charts) are photographed by sectioning the original, beginning at the upper left-hand corner and continuing from left to right in equal sections with small overlaps. Each oversize page is also filmed as one exposure and is available, for an additional charge, as a standard 35mm slide or as a 17"x 23" black and white photographic print.

Most photographs reproduce acceptably on positive microfilm or microfiche but lack the clarity on xerographic copies made from the microfilm. For an additional charge, 35mm slides of 6"x 9" black and white photographic prints are available for any photographs or illustrations that cannot be reproduced satisfactorily by xerography.



**Order Number 8718334**

**Best approximate impulse response estimate in pseudo-random  
binary sequence system identification with application to sodium  
nitroprusside pharmacodynamics**

**Jacobs, James Ralph, Ph.D.**

**The University of Alabama in Birmingham, 1987**

**Copyright ©1987 by Jacobs, James Ralph. All rights reserved.**

**U·M·I**  
300 N. Zeeb Rd.  
Ann Arbor, MI 48106



**PLEASE NOTE:**

In all cases this material has been filmed in the best possible way from the available copy. Problems encountered with this document have been identified here with a check mark .

1. Glossy photographs or pages \_\_\_\_\_
2. Colored illustrations, paper or print \_\_\_\_\_
3. Photographs with dark background \_\_\_\_\_
4. Illustrations are poor copy \_\_\_\_\_
5. Pages with black marks, not original copy \_\_\_\_\_
6. Print shows through as there is text on both sides of page \_\_\_\_\_
7. Indistinct, broken or small print on several pages
8. Print exceeds margin requirements \_\_\_\_\_
9. Tightly bound copy with print lost in spine \_\_\_\_\_
10. Computer printout pages with indistinct print \_\_\_\_\_
11. Page(s) \_\_\_\_\_ lacking when material received, and not available from school or author.
12. Page(s) \_\_\_\_\_ seem to be missing in numbering only as text follows.
13. Two pages numbered \_\_\_\_\_. Text follows.
14. Curling and wrinkled pages \_\_\_\_\_
15. Dissertation contains pages with print at a slant, filmed as received \_\_\_\_\_
16. Other \_\_\_\_\_  
\_\_\_\_\_  
\_\_\_\_\_

University  
Microfilms  
International



BEST APPROXIMATE IMPULSE RESPONSE ESTIMATE IN PSEUDO-RANDOM  
BINARY SEQUENCE SYSTEM IDENTIFICATION WITH APPLICATION TO  
SODIUM NITROPRUSSIDE PHARMACODYNAMICS

by

JAMES RALPH JACOBS

A DISSERTATION

Submitted in partial fulfillment of the requirements for the  
degree of Doctor of Philosophy in the Department of  
Biomedical Engineering in the Graduate School,  
The University of Alabama at Birmingham

BIRMINGHAM, ALABAMA

1987

Copyright by  
James Ralph Jacobs  
1987

ABSTRACT OF DISSERTATION  
GRADUATE SCHOOL, UNIVERSITY OF ALABAMA AT BIRMINGHAM

Degree Ph. D. Major Subject Biomedical Engineering

Name of Candidate James Ralph Jacobs

Title BEST APPROXIMATE IMPULSE RESPONSE ESTIMATE IN PSEUDO-RANDOM  
BINARY SEQUENCE SYSTEM IDENTIFICATION WITH APPLICATION TO  
SODIUM NITROPRUSSIDE PHARMACODYNAMICS

Crosscorrelating a pseudo-random binary input and the resulting output of a linear system provides an estimate of the impulse response function of the system. This is the well-known system identification technique of pseudo-random binary sequence testing. Most mathematical formulations of pseudo-random binary sequence system identification treat the system input and output as continuous signals, but generally in practice these signals are sampled and digitized so that the crosscorrelation and subsequent analyses can be performed using a digital computer. Modification of the impulse response estimate for the effects of sampling when it is to be used in numerical convolution was investigated in the present research. The vector containing the elements of the crosscorrelation sequence is shown to be equal to the product of a square ( $N \times N$ ) circulant matrix composed of the elements of the autocorrelation of the sampled input pseudo-random binary sequence. Multiplication of the crosscorrelation vector by

the generalized inverse of the circulant matrix, computed by two N-point discrete Fourier transforms and N reciprocations, yields the best approximate (in the least-squares sense) impulse response estimate. Computation of the best approximate solution adjusts the crosscorrelation for the effects of sampling (normalization can be substantially accomplished by dividing the crosscorrelation by the number of samples taken per state of the binary input) and, moreover, forms the best approximate numerical deconvolution of the system response to the pseudo-random binary input. Best approximate impulse response estimates were calculated for data obtained from measuring the hemodynamic effects of pseudo-random binary infusions of sodium nitroprusside in six dogs. Convolution of the input sequence for each dog with the best approximate impulse response estimate for eleven variables resulted in sequences with mean-square errors (compared with the actual hemodynamic data) one or two orders of magnitude smaller than did convolution with a normalized crosscorrelation estimate. The best approximate impulse response estimate is a powerful enhancement to pseudo-random binary sequence testing; its greatest utility may be in black-box simulation studies, but the prospect also exists to separate the dynamic and background components of the system response.

Abstract Approved by: Committee Chairman

Rui C. Shoppard

Program Director

Rui C. Shoppard

Date

3/6/87

Dean of Graduate School

Cathary Hamad

## ACKNOWLEDGEMENTS

My gratitude to Dr. Louis C. Sheppard for his support during my tenure as a graduate student in his department is exceeded only by reverence for his already classic contributions to biological systems analysis and therapeutic automation. Dr. Sheppard's own doctoral studies pioneered the groundwork upon which this dissertation is based.

With Dr. Sheppard's enthusiastic cooperation, much of this research was performed at Duke University Medical Center, where Dr. J. Gerald Reves has been my mentor and sponsor; he has my eternal thanks and veneration. Dr. Reves and the Duke Department of Anesthesiology through Dr. W. David Watkins have placed virtually unlimited resources at my disposal with which to pursue this and other research. The animal experiments reported here were possible only through the gracious generosity of Dr. J. Scott Rankin, a zealous and brilliant man for whom I have much regard. Dr. George W. Maier brought invaluable technical and intellectual assistance to these dog studies.

Friendship with my colleague Eric D. Hawkins ultimately inspired me to spend the final hours necessary to identify this manuscript from the incessant background noise of other

responsibilities that always seemed to take priority. This dissertation is dedicated, with love and respect and appreciation to my parents, Ralph M. and Rickey G. Jacobs.

## TABLE OF CONTENTS

	<u>Page</u>
ACKNOWLEDGEMENTS.....	v
LIST OF TABLES.....	viii
LIST OF FIGURES.....	ix
LIST OF ABBREVIATIONS.....	xii
CHAPTER 1: INTRODUCTION.....	1
CHAPTER 2: PRB TESTING AND THE BEST APPROXIMATE SOLUTION.....	6
2.1 PRB Testing - Implementation.....	6
2.2 Properties of Sampled PRB Signals.....	10
2.3 PRB Testing with Sampled Signals.....	17
2.4 Sampled PRB Testing - Best Approximate Solution.....	19
2.5 Multidimensional Sampled PRB Testing.....	23
CHAPTER 3: EXPERIMENTAL VERIFICATION.....	26
3.1 Methods - Animal Experiments.....	26
3.2 Methods - Data Analysis.....	31
CHAPTER 4: RESULTS.....	40
CHAPTER 5: DISCUSSION.....	71
LIST OF REFERENCES.....	82
APPENDICES:	
A: Circulant Inversion.....	87
B: Simulation of Closed-loop Nitroprusside.....	89

LIST OF TABLES

<u>Table</u>	<u>Page</u>
4-1	Means and linear regression parameters for sampled hemodynamic data sequences. Units are given for the mean and y-intercept. Slope is in units of $\Delta \text{unit} \cdot \Delta \text{minute}^{-1}$ ..... 41
4-2	Correlation between the average crosscorrelation impulse response estimate and each individual estimate for each variable.. 51
4-3	Correlation between the average best approximate impulse response estimate and each individual best approximate estimate for each variable..... 52
4-4	Mean-square errors between data sequences and model sequences. Averages are $\text{mean} \pm \text{S.D.}$ , $n=6$ . Model sequences for each dog for each variable were computed by convolving each of the impulse response types with its corresponding sampled PRB signal..... 60
4-5	Baroreceptor reflex control of heart rate analyzed using impulse response estimates. Data were derived from three types of impulse response estimates: A-crosscorrelation estimate, B-filtered crosscorrelation estimate, C-filtered best approximate estimate..... 64

## LIST OF FIGURES

<u>Figure</u>	<u>Page</u>
2-1 Schematized linear system. The continuous linear system $h_c(t)$ produces an output signal $y_c(t)$ when perturbed by an input signal $x_c(t)$ .....	7
2-2 PRB test signal. Schematic representation of an m-state PRB signal of amplitude $\pm\alpha$ with a switching interval of $\lambda$ seconds.....	8
2-3 Autocorrelation of sampled PRB signal. Parameters are as defined in figure 2-2, with s being the number of samples taken per state of the PRB signal.....	12
2-4 Time-shifted autocorrelation of sampled PRB signal. Compare with figure 2-3.....	14
4-1 Blood pressure and heart rate data from one dog during PRB nitroprusside infusion. Legend: 1-schematic representation of nitroprusside infusion signal; 2-heart rate; 3-systolic, 4-mean, 5-diastolic arterial pressure; 6-mean LV ejection pressure. Units: 1-high=pump on, low=pump off; 2-bpm; 3 through 6-mm Hg.....	42
4-2 Non-normalized crosscorrelation estimate. Example from one dog for mean arterial pressure...	43
4-3 Normalized, time-shifted crosscorrelation estimate. Example from one dog for mean arterial blood pressure.....	44
4-4 Average normalized crosscorrelation estimates for heart rate and LV ejection and arterial pressures.....	46
4-5 Average normalized crosscorrelation estimates for end-diastolic pressure and minor axis diameter....	47

LIST OF FIGURES (continued)

<u>Figure</u>	<u>Page</u>
4-6 Average normalized crosscorrelation estimates for positive and negative LV dP/dt.....	48
4-7 Average normalized crosscorrelation estimates for ejection shortening and stroke work. Stroke work estimate was multiplied by 100 for convenience in plotting.....	49
4-8 Convolution with non-normalized crosscorrelation. Line represents convolution estimate for mean arterial pressure from one dog.....	53
4-9 Convolution with normalized crosscorrelation. Example from one dog for mean arterial pressure. Crosses represent actual data during PRB nitroprusside infusion. Solid line represents convolution of the PRB sequence with the normalized crosscorrelation impulse response estimate (cf. figure 4-8).....	54
4-10 First row of generalized inverse of autocorrelation matrix. The generalized inverse of the autocorrelation matrix for the PRB sequence used in this study was an 1827x1827 circulant matrix.....	56
4-11 Best approximate impulse response estimate. Time-shifted example from one dog for mean arterial pressure (cf. figure 4-3).....	57
4-12 Convolution with best approximate impulse response. The model tracing is an example from one dog of convolution of the PRB sequence with the best approximate impulse response estimate for mean arterial pressure. Shown below it for reference (amplitude-shifted for clarity) is the actual data sequence.....	58
4-13 Comparison of normalized crosscorrelation and filtered best approximate impulse response estimate. Example from mean arterial pressure in one dog. Both sequences are time-shifted. The best approximate estimate is the smoother curve with a positive y-intercept.....	59

LIST OF FIGURES (continued)

<u>Figure</u>	<u>Page</u>
4-14 Sample computation of response time for baroreceptor heart rate response. Dark data points are those used in linear regression analysis (solid line) to determine x-intercept....	62
4-15 Sample computation of baroreceptor heart rate response gain. Dark data points are those used in linear regression analysis (solid lines) to determine activation and deactivation gains.....	63
4-16 Simulation of closed-loop nitroprusside infusion: arterial pressure and heart rate response. Setpoint for mean arterial pressure (controlled variable) was 75 mm Hg.....	65
4-17 Simulation of closed-loop nitroprusside infusion: nitroprusside dose and LV end-diastolic pressure response. Lower tracing: nitroprusside (SNP) infusion rates specified by the control algorithm to achieve the setpoint mean arterial pressure....	66
4-18 Simulation of closed-loop nitroprusside infusion: positive and negative LV dP/dt response.....	67
4-19 Simulation of closed-loop nitroprusside infusion: stroke work response.....	68
4-20 Simulation of closed-loop nitroprusside infusion: ejection shortening response.....	69

## LIST OF ABBREVIATIONS

bpm	Beats per Minute
DAP	Diastolic Arterial Pressure
dP/dt	Time-rate-of-change of Pressure
DPN	Peak Negative LV dP/dt
DPP	Peak Positive LV dP/dt
EJS	LV Minor Axis Ejection Shortening
EDL	LV Minor Axis End-diastolic Diameter
EDP	LV End-diastolic Pressure
HR	Heart Rate
LV	Left Ventricular
MAP	Mean Arterial Pressure
MEP	Mean LV Ejection Pressure
PRB	Pseudo-random Binary
SAP	Systolic Arterial Pressure
SNP	Sodium Nitroprusside
SW	LV Minor Axis Stroke Work

## CHAPTER 1

### INTRODUCTION

The impulse response function constitutes a complete functional description of the input-output relation of a linear system. Because of the vital role that the impulse response function plays in system simulation and in control system design, identification of the impulse response function has been intensively investigated. Methods for obtaining the impulse response range from direct observation of the system output resulting from an impulsive input to sophisticated Kalman filtering algorithms.

One popular system identification technique [DA-70] is known as pseudo-random binary sequence testing (PRB testing), wherein an estimate of the linear or linearized system's impulse response function is obtained by computing the crosscorrelation function between a PRB input and the resulting system output. The subject of this report is enhancement of PRB testing by considering the effects of periodic sampling of the input and output signals on the crosscorrelation computation. Clearly, in most contemporary applications of PRB testing the crosscorrelation and subsequent analyses will be performed using a digital

computer, necessitating digitized sample estimates of the input/output signals, but it is not apparent that the effect of sampling on the impulse response estimate obtained by crosscorrelation has been considered previously.

The ideal test signal, such as white noise or a Dirac pulse, for use in identifying the impulse response function would have flat power spectra from minus to plus infinity to excite equally all possible modes of the system under investigation [EY-74]. However, these ideal probe signals can be realized and utilized only with great difficulty, if at all. PRB sequences have properties that are in themselves desirable, as well as approximating those of the ideal test signals, and as such PRB sequences have found utility in system identification.

The name pseudo-random intimates a test signal with properties similar to white noise, but that is deterministic [DA-70, RU-73]. A PRB sequence is periodic and over a single period has a triangular autocorrelation function; that this autocorrelation function approximates an impulse is indicative of the white noise characteristics of the PRB sequence. A further advantage of this test signal is that the amplitude of the pseudo-random stimulus need be only large enough to induce a measurable response from the system under study. As summarized by Slate [SL-80], PRB testing permits the injection of a relatively large amount of energy over a specified period of time using a relatively small amplitude input signal, and hence the signal-to-noise ratio is improved while nonlinearities associated with large-

signal input perturbations are avoided.

Examples of the application of PRB testing include identification of a binary distillation column [UR-86], measurement of the dynamic thermal response in rooms [LE-82], and identification of a gas-turbine engine [GO-74]. Gufstavsson [GU-75] gives a survey of applications of PRB testing in the identification of chemical and physical processes. Several authors have extolled the benefits of PRB testing [BU-77, DA-70, GO-80, GU-75, LI-81, PO-74a], while others [BU-81] have noted antipathy toward PRB testing, at least with regard toward PRB excitation as a multifrequency test signal.

Biological systems are notoriously susceptible to large-signal input nonlinearities [MA-78], and therefore many investigators have been attracted to PRB testing because of the relatively small magnitude input perturbation that this method exploits. Furthermore, PRB testing usually requires a much shorter measurement period than does direct sinusoidal testing, a critical consideration in the analysis of biological systems that do not remain stationary for extended lengths of time. Finally, biological systems are characteristically noisy, and the signal averaging inherent in the crosscorrelation computation helps PRB testing to achieve impulse response measurements with desirable signal-to-noise properties.

Toll [TO-73] measured the crosscorrelation between pseudo-random variations of extracellular calcium concentration and the response of peak isometric tension of

an isolated heart muscle in a study of myocardial inotropism. Rubenstein, Kenner, and Ono [RU-73] used PRB testing to investigate the low frequency properties of renal and femoral hemodynamic variables. Ponte and Purves [PO-74a, 74b] proposed PRB testing to measure the frequency response of sensory receptors. Poussart and Ganguly [PO-77] used PRB testing in kinetic studies of ionic processes in nerve membrane. Giard et al. [GI-85] used PRB testing to identify the oxygen and carbon dioxide responses in an artificial ventilation system. Sheppard et al. [SH-76, 77, 80, 82] and Linkens et al. [LI-81, 82] used PRB drug infusions to characterize dynamic pharmacodynamics.

Although in a number of the papers mentioned above [GI-85, GO-74, 80, LE-82, LI-82, PO-74, 77, RU-73, SH-76, 77] specific reference is made to digital computation of the crosscorrelation impulse response estimate, in none is discussed the effect, if any, on the crosscorrelation of sampling of the PRB input and the system output. This is surprising considering the attention given to sampling in most digital signal processing texts [EY-74, OP-75], but is probably founded in the fact that these authors used the PRB testing-derived impulse response estimates as an approximation to the continuous system function and did not perform digital simulations, where the effects of sampling become critical.

In casual computer simulations of linear (and nonlinear) system identification by PRB testing, sampling rate-dependent scaling of sequences obtained by convolving

the derived discrete system function estimate with the PRB sequence used to generate it was observed; the shape of these convolution sequences was as expected, but gross amplitude distortion occurred. Therefore, it became the objective of this research to develop a systematic approach to compensate for the effects of input/output sampling when the impulse response estimate obtained by PRB testing is to be used in numerical convolutions. A technique to compute the best approximate impulse response estimate was developed and applied to pharmacodynamic identification of the canine hemodynamic response to sodium nitroprusside.

## CHAPTER 2

### PRB TESTING AND THE BEST APPROXIMATE SOLUTION

The quintessential reference on pseudo-random binary sequence testing is a text by Davies [DA-70]. Among other general treatments of PRB testing are excellent papers by Godfrey [GO-80] and Isermann [IS-80] and texts by Marmarelis and Marmarelis [MA-78] and Eykhoff [EY-74]. Barker and Davy [BA-75] describe system identification using PRB signals and the discrete Fourier transform. Golomb [GO-82] gives a thorough exposition on the mathematics of PRB sequences. Clarke and Briggs [CL-70a, 70b] consider the effects of contaminating noise in PRB testing.

In this Chapter, the mathematics of discrete PRB system identification are developed and some of the properties of sampled PRB signals are listed. The best approximate discrete impulse response estimate is derived and an attempt is made to generalize this result to multidimensional PRB testing.

#### 2.1 PRB Testing - Implementation

A linear or linearized system (figure 2-1) with impulse response  $h_c(t)$  is stimulated by a periodic pseudo-random binary signal [DA-70, SH-76]  $x_c(t)$  (figure 2-2) with  $m$  states of amplitude  $\pm\alpha$  of duration  $\lambda$ , producing an output

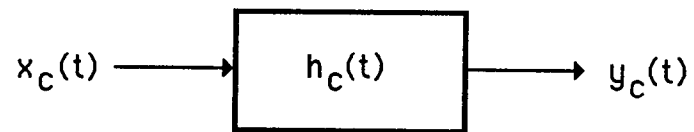


Figure 2-1. Schematized linear system. The continuous linear system  $h_c(t)$  produces an output signal  $y_c(t)$  when perturbed by an input signal  $x_c(t)$ .

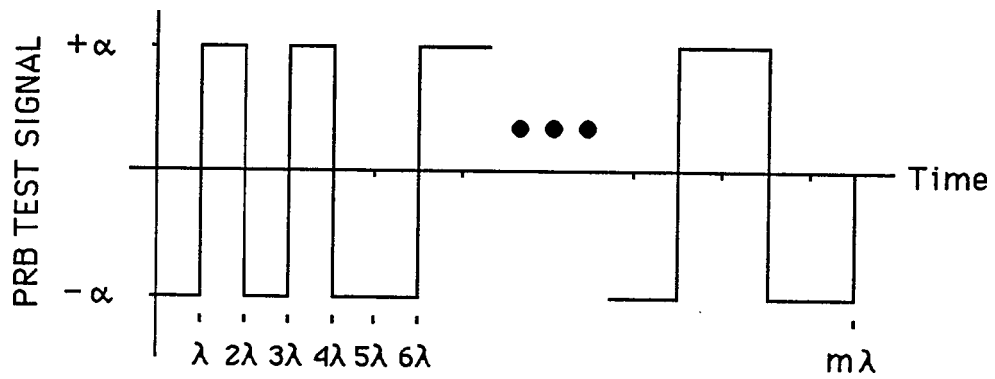


Figure 2-2. PRB test signal. Schematic representation of an  $m$ -state PRB signal of amplitude  $\pm\alpha$  with a switching interval of  $\lambda$  seconds.

signal  $y_c(t)$ . The subscript  $c$  denotes a continuous waveform and  $t$  is time.

Generation of  $m$ -state PRB sequences [DA-70] is easily realized in hardware or software and effectively results in a sequence of  $m$  ones and zeros. A PRB sequence is obviously defined as a sequence, but conversion to a continuous waveform, conceptualized as convolution of each Dirac pulse in the PRB sequence with a rectangular window, preserves its essential characteristics and allows it to be treated as a signal [SH-76], which is a pragmatic and theoretical necessity if a continuous system is to be identified. The usual convention is to relate the ones to a level of  $+\alpha$  and the zeros to a level of  $-\alpha$ .

Parameters  $m$  and  $\lambda$  are chosen [SH-76] to give  $x_c(t)$  the bandwidth required to identify  $h_c(t)$ , where the  $-3\text{dB}$  bandwidth of a PRB sequence is  $1/m\lambda$  to  $1/3\lambda$  [DA-70]. The impulse response  $h_c(t)$  is assumed to decay to zero within the period  $m\lambda$ , and the system is assumed to be stationary for a period of at least  $2m\lambda$ , the minimum duration of the identification process. Further, it may be necessary to add an offset to  $x_c(t)$  to bias the system into its linear operating range.

The system is excited by  $x_c(t)$  at least twice consecutively; the first stimulation period is used to bring the system into dynamic steady-state before data collection begins, at the start of the second stimulation period [SH-76, BU-77]. If the system remains stationary, additional

contiguous excitation periods may be administered when serial impulse response estimates are desired.

Sequences  $x(n)$  with values  $x_c(n\delta)$  and  $y(n)$  with values  $y_c(n\delta)$  are derived from  $x_c(t)$  and  $y_c(t)$  ( $n=0,1,2,\dots,N-1$ ), respectively, by periodic sampling with sampling period  $\delta$ . The sampling period  $\delta$  is chosen such that there are an integral number  $s$  ( $s>1$ ) of samples (guaranteed to be well above the Nyquist rate) taken per state of the input PRB signal. The objective, then, is to derive from the sequences  $x(n)$  and  $y(n)$  of length  $N$ , where  $N\delta=m\lambda$ , a discrete estimate  $h(n)$  of  $h_c(t)$ .

## 2.2 Properties of Sampled PRB Signals

Davies [DA-70] provides an extensive treatise on the properties of PRB sequences. However, sampling of the signal as described in Section 2.1 will result in what is effectively a sampled PRB sequence or, more appropriately, a sampled PRB signal. Discussed in this section are some of the relevant properties of a sequence obtained from sampling (under the constraints imposed in Sec. 2.1) a PRB signal.

- 1) A PRB sequence is of length  $m=2^n-1$ , where  $n\geq 3$  is an integer. Therefore, the length of the sequence obtained from sampling one period of a PRB signal will be  $N=s(2^n-1)$ .
- 2) The sequence of length  $N$  obtained from sampling one period of a PRB signal will contain  $(N+s)/2 + \alpha$  elements and  $(N-s)/2 - \alpha$  elements. Thus, in one period, the number of

$+\alpha$  elements will exceed the number of  $-\alpha$  elements by  $s$ . As a consequence, the average value of the sequence will be  $s\alpha/N$ .

- 3) The autocorrelation sequence  $\phi_{xx}(n)$  for the elements of the sequence obtained from sampling one period of a PRB signal is shown graphically in figure 2-3. Explicitly,  $\phi_{xx}(n)$  can be expressed

$$\phi_{xx}(n) = \begin{cases} \alpha^2 \left[ 1 - \frac{n}{ms} - \frac{n}{s} \right] & 0 \leq n \leq s \\ -\frac{\alpha^2}{m} & s+1 \leq n \leq (m-1)s-1 \\ \alpha^2 \left[ -m + \frac{n}{ms} + \frac{n}{s} \right] & (m-1)s \leq n \leq ms-1 \end{cases} \quad (2-2-1)$$

where  $\alpha$  and  $m$  are as defined in figure 2-2,  $s$  is the number of samples per state of the PRB signal, and  $ms=N$ .

Since sampled PRB sequences are periodic in  $N$ , their autocorrelation sequences are periodic in  $N$ . The sequence in figure 2-3 could equally well have been plotted from  $n=-s$  to  $(m-1)s-1$  in which case the triangular portion of the sequence would be centered over  $n=0$ . However,  $n$  is generally related in some way to time, so manipulation of sequence index numbers ( $n$ ) less than zero is usually avoided,

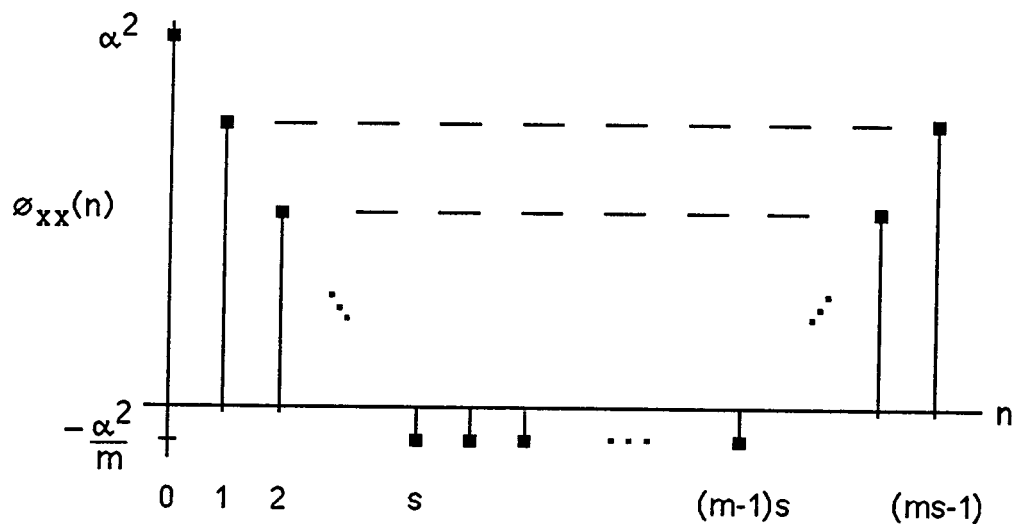


Figure 2-3. Autocorrelation of sampled PRB signal. Parameters are as defined in figure 2-2, with  $s$  being the number of samples taken per state of the PRB signal.

and hence half of the triangular portion of the autocorrelation is revealed at the end of the sequence  $\phi_{xx}(n)$  since it has been calculated and displayed from  $n=0$  to  $N-1$ .

The autocorrelation sequence  $\phi_{xx}(n)$  is a measure of the dependence between values of the sampled pseudo-random sequence at different times  $n\delta$  and in this sense describes the time variation of the sequence [OP-75]. Since in PRB testing the objective is to identify the impulse response, or system response to an impulsive input, the sequence  $\phi_{xx}(n)$  should be time-shifted by  $s$  elements and wrapped around (see figure 2-4) to better approximate an impulsive autocorrelation over the period  $n=0$  to  $N-1$ . Sheppard [SH-76] was probably the first to recognize this, but the procedure was not discussed.

The practical consequence of this observation is that just as with the autocorrelation, sequences obtained from other operations such as crosscorrelation or convolution with the sampled PRB sequence must be time-shifted by  $s$  and wrapped around for proper representation as a temporal sequence; subsequent reference in this report to a time-

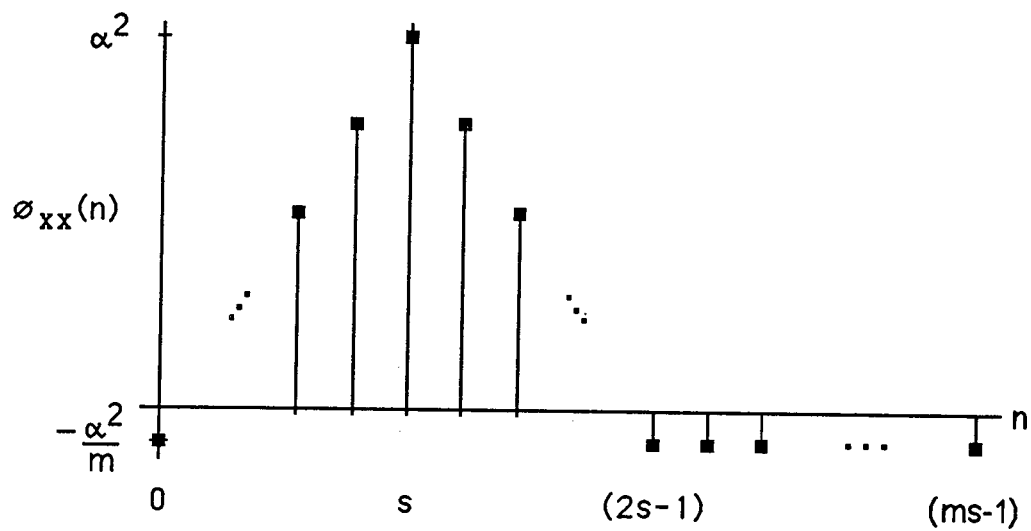


Figure 2-4. Time-shifted autocorrelation of sampled PRB signal. Compare with figure 2-3.

shifted sequence will mean a sequence so treated.

- 4) Crosscorrelating a sampled periodic PRB signal with amplitude  $\pm\alpha$  with a delayed, the delay being an integral number  $p$  of binary states of the continuous signal, version of itself but with amplitude  $\pm\beta$  results in a sequence of the form shown in figure 2-3 for the autocorrelation sequence, except that the triangular portion of the sequence will be shifted by  $ps$  and the peak amplitude will be  $\alpha\beta$ . Thus the two sequences are relatively uncorrelated for lags up to  $(p-1)s$ . This point becomes significant in multidimensional PRB testing.
- 5) The power spectrum  $\Phi(\omega)$  of a periodic PRB signal has been stated incorrectly by Easterling [EA-64] and Davies [DA-70]. Lamb [LA-70] has correctly given the following equation as the power spectrum of a PRB signal with  $m$  states of amplitude  $\pm 1$  and clock period  $\lambda$ , disregarding the dc term:

$$\Phi(\omega) = \frac{m+1}{m} \left[ \frac{\sin(\omega\lambda/2)}{\omega\lambda/2} \right]^2 \sum_{\substack{n=-\infty \\ n \neq 0}}^{\infty} \delta\left(\omega - \frac{2\pi n}{\lambda}\right)$$

(2-2-2)

where  $\delta(x)$  is the unit impulse function. This power spectrum has an envelope proportional to  $[\sin(\omega\lambda/2)/(\omega\lambda/2)]^2$ , with spectral lines occurring at  $2\pi/m\lambda$ ,  $4\pi/m\lambda$ , etc., for  $\omega > 0$ . The first node is at  $\omega = 2\pi/\lambda$ . As mentioned previously, the effective bandwidth of the test signal is from  $2\pi/m\lambda$  to  $2\pi/3\lambda$  rad/sec.

The sequence of the power spectrum estimates  $\Phi_N(\omega)$ , as computed using the discrete Fourier transform, of the sequence derived by sampling one period of a PRB signal of amplitude  $\pm\alpha$  can be stated as

$$\Phi_N(\omega) = \frac{\alpha^2 s(m+1)}{m} \left[ \frac{\sin(\omega\lambda/2)}{\omega\lambda/2} \right]^2 \sum_{n=1}^{\infty} \delta\left(\omega - \frac{2\pi n}{N\delta}\right) \quad (2-2-3)$$

where, as before,  $s$  ( $s > 1$ )  $= \lambda/\delta$  is the number (integer) of samples taken per state of the PRB signal,  $\delta$  is the sampling interval, and  $N\delta = m\lambda$ . The point to be made here is that this spectrum is amplified by  $s$ , and therefore the impulse response estimate derived by crosscorrelation must be normalized by dividing each element in the sequence by  $s$  when a discrete input sequence is to be convolved with the model impulse response

estimate to obtain a discrete simulation of the system response to the perturbation.

### 2.3 PRB Testing with Sampled Signals

Define the sequence  $y_0(n)$  as  $y(n)$  minus the average of  $y(n)$  for  $n=0,1,2,\dots,N-1$ . The periodic sequences  $y_0(n)$  and  $x(n)$  are related by the convolution sequence

$$y_0(n) = \sum_{k=-\infty}^{\infty} h(k) x(n-k) \quad (2-3-1)$$

The crosscorrelation sequence  $\phi_{xy}(n)$  between the sampled system input and output is defined as

$$\phi_{xy}(n) = \frac{1}{N} \sum_{p=0}^{N-1} x(p) y_0(p+n) \quad (2-3-2)$$

Substituting into equation (2-3-2) the definition for  $y_0(n)$  given by equation (2-3-1) yields

$$\phi_{xy}(n) = \frac{1}{N} \sum_{p=0}^{N-1} x(p) \sum_{k=-\infty}^{\infty} h(k) x(p+n-k) \quad (2-3-3)$$

which upon exchanging the order of summation becomes

$$\phi_{xy}(n) = \sum_{k=-\infty}^{\infty} h(k) \left[ \frac{1}{N} \sum_{p=0}^{N-1} x(p) x(p+n-k) \right] \quad (2-3-4)$$

The expression within brackets in equation (2-3-4) is the autocorrelation sequence  $\phi_{xx}(n-k)$ , and thus

$$\phi_{xy}(n) = \sum_{k=-\infty}^{\infty} h(k) \phi_{xx}(n-k) \quad (2-3-5)$$

Since  $h(k)=0$  for  $k<0$  and since  $h(k)$  decays to zero within the period  $N\delta$  (see Section 2.1), equation (2-3-5) may be rewritten as

$$\phi_{xy}(n) = \sum_{k=0}^{N-1} h(k) \phi_{xx}(n-k) \quad (2-3-6)$$

The derivation to this point is analogous to that given by Davies [DA-70] for continuous signals.

In matrix notation, equation (2-3-6) can be expressed as

$$\begin{bmatrix} \phi_{xy}(0) \\ \phi_{xy}(1) \\ \vdots \\ \phi_{xy}(N-1) \end{bmatrix} = \begin{bmatrix} \phi_{xx}(0) & \phi_{xx}(1) & \cdots & \phi_{xx}(N-1) \\ \phi_{xx}(N-1) & \phi_{xx}(0) & \cdots & \phi_{xx}(N-2) \\ \vdots & \vdots & \ddots & \vdots \\ \phi_{xx}(1) & \phi_{xx}(2) & \cdots & \phi_{xx}(0) \end{bmatrix} \begin{bmatrix} h(0) \\ h(1) \\ \vdots \\ h(N-1) \end{bmatrix} \quad (2-3-7)$$

or more compactly as

$$\phi_{xy} = \phi_{xx}h \quad (2-3-8)$$

Classically, the approximation is made that  $\phi_{xx}(k)=0$  for

$k=1,2,3,\dots,N-1$  (i.e., that the autocorrelation sequence of the sampled input PRB signal is equal to zero except for an impulse at  $k=0$  where  $\phi_{xx}(0)=\alpha^2$ ), in which case  $\phi_{xx}$  is equal to the scaled  $N \times N$  identity matrix  $\alpha^2 \mathbf{I}$ . Then,

$$\phi_{xy} = \phi_{xx} \mathbf{h} \approx \alpha^2 \mathbf{I} \mathbf{h} = \alpha^2 \mathbf{h} \quad (2-3-9)$$

This result states that the scaled crosscorrelation sequence between a sampled input PRB signal and the resulting sampled system output sequence is approximately equal to the scaled impulse response sequence. Equation (2-3-9) forms the basis for PRB testing as it is usually performed, with  $\phi_{xy}(n)$  computed by equation (2-3-2). Clearly, by property 3 in Section 2.2, the assumption that all of the off-diagonal elements of  $\phi_{xx}$  are zero can be a very coarse approximation, potentially resulting in significant distortion of the impulse response sequence derived from the input/output crosscorrelation. In the following section the best approximate solution in PRB testing is derived by utilizing the autocorrelation sequence to its full accuracy.

#### 2.4 Sampled PRB Testing - Best Approximate Solution

Examining equation (2-3-8), if the inverse  $\phi_{xx}^{-1}$  of  $\phi_{xx}$  can be formed, then the exact solution  $\mathbf{h}$  is determined by simply multiplying both sides of equation (2-3-8) by  $\phi_{xx}^{-1}$ :

$$\phi_{xx}^{-1} \phi_{xx} \mathbf{h} = \mathbf{I} \mathbf{h} = \mathbf{h} = \phi_{xx}^{-1} \phi_{xy}.$$

The inverse of a general matrix is not necessarily defined, though, and in practical application,  $\phi_{xx}$  can contain many tens of thousands of elements, making inversion computationally difficult, if not impossible, even if it does exist. It will be shown that  $\phi_{xx}^{-1}$  does not exist but that the best approximate solution  $\mathbf{h}' = \phi_{xx}^+ \phi_{xy}$ , where  $\phi_{xx}^+$  is the generalized inverse of  $\phi_{xx}$ , can be easily computed.

By inspection of the  $N \times N$  matrix  $\phi_{xx}$  it is observed that the elements of each row are identical to those of the previous row moved one position to the right and wrapped around. A matrix of this form is known as a circulant [DA-79], and it is apparent that the whole circulant is determined by the first row so that  $\phi_{xx}$  can be expressed  $\phi_{xx} = \text{circ}[\phi_{xx}(0), \phi_{xx}(1), \dots, \phi_{xx}(N-1)]$ , where  $\text{circ}[x]$  denotes an  $N \times N$  matrix of the form just described. Obviously, the elements of the first row of  $\phi_{xx}$  are simply the elements of the autocorrelation sequence (equation 2-2-1) of the sampled input PRB signal.

The eigenvalues  $\lambda_j$  of a circulant matrix are defined [DA-79] as the scaled inverse discrete Fourier transform of the first row elements of the circulant. Since the sequence  $\phi_{xx}(n)$  is triangular, the inverse Fourier transform will take the form of a sinc function and every  $m$ -th element will equal zero. Therefore,  $\phi_{xx}$  is not full rank and cannot be explicitly inverted, and the exact solution of equation (2-3-8) cannot necessarily be computed. However, the

generalized inverse of  $\Phi_{xx}$  can be formed, and from this the best approximate solution [GR-83] computed.

A circulant matrix  $\mathbf{C}$  is diagonalized [DA-79] by the Fourier matrix  $\mathbf{F}$  so that  $\mathbf{C} = \mathbf{F}^* \Lambda_{\mathbf{C}} \mathbf{F}$ , where  $*$  denotes the conjugate transpose and  $\Lambda_{\mathbf{C}} = \text{diag}[\lambda_{\mathbf{C}0}, \lambda_{\mathbf{C}1}, \lambda_{\mathbf{C}2}, \dots, \lambda_{\mathbf{C}(N-1)}]$ . The Fourier matrix is defined [GR-83] as a  $k \times k$  matrix with every  $pq$ -th element equal to  $k^{-1/2} \omega^{(p-1)(q-1)}$  with  $\omega = \cos 2\pi/k - j \sin 2\pi/k$  and  $j = \sqrt{-1}$ . The Moore-Penrose generalized inverse  $\mathbf{C}^+$  of  $\mathbf{C}$  is the  $N \times N$  circulant [DA-79]

$$\mathbf{C}^+ = \mathbf{F}^* \Lambda_{\mathbf{C}}^+ \mathbf{F}, \quad (2-4-1)$$

where  $\Lambda_{\mathbf{C}}^+ = \text{diag}[\lambda_{\mathbf{C}0}^+, \lambda_{\mathbf{C}1}^+, \lambda_{\mathbf{C}2}^+, \dots, \lambda_{\mathbf{C}(N-1)}^+]$  with

$$\begin{cases} \lambda_i^+ = \frac{1}{\lambda_i} & \text{for scalar } \lambda_i \neq 0 \\ \lambda_i^+ = 0 & \text{for scalar } \lambda_i = 0 \end{cases} \quad (2-4-2)$$

Finally, let  $\mathbf{C} = \text{circ } \gamma$  and  $\mathbf{C}^+ = \text{circ } \gamma^+$ ; it can be shown [DA-79] that

$$(\gamma^+)^T = \mathbf{F}(\mathbf{F}^* \gamma^T)^+, \quad (2-4-3)$$

where  $\gamma^T$  is the transpose of  $\gamma$ . From equations (2-4-3) and (2-4-2) it appears that the generalized inverse of a circulant can be computed in 2  $N$ -point discrete Fourier transforms plus  $N$  reciprocations.

In the context of PRB testing,

$$[\phi_{xx}(0)^+ \phi_{xx}(1)^+ \phi_{xx}(2)^+ \dots \phi_{xx}(N-1)^+]^T =$$

$$\mathbf{F}\{\mathbf{F}^*[\phi_{xx}(0) \phi_{xx}(1) \phi_{xx}(2) \dots \phi_{xx}(n-1)]^T\}^+$$

(2-4-4)

Algorithmically, the elements  $\phi_{xx}(n)^+$  for  $n=0,1,2,\dots,N-1$  of the first row of the circulant  $\phi_{xx}^+$  (and thence the entire  $N \times N$  matrix  $\phi_{xx}^+$ ) are computed by finding the inverse discrete Fourier transform of the elements of the first row of  $\phi_{xx}$ , performing on this sequence the transformation of equation (2-4-2), and then computing the forward discrete Fourier transform of the result. Note that since the autocorrelation sequence is always even, the elements of the inverse discrete Fourier transform of  $\phi_{xx}(n)$  are all real.

Given the system  $\mathbf{AX} = \mathbf{B}$ , the vector  $\mathbf{A}^+\mathbf{B}$  always exists and is either the unique least squares solution or it is the solution of minimum norm [PE-55, GR-83], and this is by definition the best approximate solution to the system  $\mathbf{AX} = \mathbf{B}$ . Therefore, the best approximate impulse response estimate in PRB testing is

$$\mathbf{h}' = \phi_{xx}^+ \phi_{xy} \quad (2-4-5)$$

## 2.5 Multidimensional Sampled PRB Testing

It may be possible to generalize the preceding discussion to the identification of the multidimensional system with  $p$  inputs and  $q$  outputs, where each output  $y_g(n)$  is related to each input  $x_i(n)$  by an impulse response sequence  $h_{ig}(n)$  [DA-70]. Each output  $y_g(n)$  is the linear sum of the effects caused on  $y_g(n)$  by each of the inputs, and more specifically, all inputs and outputs are mathematically related through the operation of convolution.

Considering a particular output  $y_g(n)$  and all inputs  $x_i(n)$ ,  $1 \leq i \leq p$ ,

$$y_g(n) = \sum_{i=1}^p \sum_{k=-\infty}^{\infty} h_{ig}(k) x_i(n-k) \quad (2-5-1)$$

The crosscorrelation sequence between a particular input  $x_k(n)$  and a particular output  $y_g(n)$  is

$$\phi_{x_k y_g}(n) = \frac{1}{N} \sum_{f=0}^{N-1} x_k(f) y_g(f+n) \quad (2-5-2)$$

Inserting the definition for  $y_g(n)$  given in equation (2-5-1) yields

$$\phi_{x_k y_g}(n) = \frac{1}{N} \sum_{f=0}^{N-1} x_k(f) \left[ \sum_{i=1}^p \sum_{k=-\infty}^{\infty} h_{ig}(k) x_i(f+n-k) \right] \quad (2-5-3)$$

which upon exchanging the order of summation becomes

$$\phi_{x_k Y_g}(n) = \sum_{i=1}^P \sum_{k=-\infty}^{\infty} h_{ig}(k) \left[ \frac{1}{N} \sum_{f=0}^{N-1} x_k(f) x_i(f+n-k) \right] \quad (2-5-4)$$

The term within brackets is by definition the crosscorrelation sequence:

$$\phi_{x_k Y_g}(n) = \sum_{i=1}^P \sum_{k=0}^{N-1} h_{ig}(k) \phi_{x_k x_i}(n-k) \quad (2-5-5)$$

noting again that the impulse response sequence need only be referenced from 0 to N-1. Finally, equation (2-5-5) can be written in matrix notation as

$$\begin{aligned} \phi_{x_k Y_g} = & \phi_{x_k x_1} h_{1g} + \phi_{x_k x_2} h_{2g} + \dots \\ & + \phi_{x_k x_k} h_{kg} + \dots + \phi_{x_k x_p} h_{pg} \end{aligned} \quad (2-5-6)$$

If  $\phi_{x_k x_i} = 0$  for  $k \neq i$ , i.e.,  $x_k(n)$  and  $x_i(n)$  are uncorrelated, then the best approximate impulse response estimate  $\mathbf{h}'_{kg}$  could be identified analogously to equation (2-4-5). Though for lags prior to the length of the delay between  $x_i(n)$  and  $x_k(n)$  the crosscorrelation  $\phi_{x_k x_i}(n)$  does have finite value ( $= -\alpha\beta/N$ ), the best result obtainable from equation (2-5-6) is to assume  $\phi_{x_k x_i} = 0$  for  $k \neq i$ , to compute  $\mathbf{h}'_{kg}$ , and to use only those elements of  $\mathbf{h}'_{kg}$  representing the interval of the shortest delay between  $x_k(n)$  and  $x_i(n)$ . It is obvious by inspection that matrix inversion techniques, and

consequently a generalization of the derivation in Section 2.4, cannot solve equation (2-5-6) for  $h_{kg}$  or  $h_{kg}'$ .

## CHAPTER 3

### EXPERIMENTAL VERIFICATION

To verify the best approximate impulse response estimation technique developed theoretically in the previous chapter, PRB identification experiments were performed to characterize the canine hemodynamic response to sodium nitroprusside. The hypothesis was that the best approximate impulse response sequence would be a better characterization of the system in numerical convolutions than the normalized (multiplied by  $s^{-1}$ ) crosscorrelation estimate, and that convolution with either of these estimates would be satisfactory, whereas convolution with the non-normalized crosscorrelation estimate is inappropriate. The basis for judging the quality of the impulse response estimate was the mean-square error between the original data sequence and the sequence generated by convolving the sampled test PRB signal with the impulse response estimates.

#### 3.1 Methods - Animal Experiments

Six adult mongrel dogs of either sex were surgically instrumented for chronic study. The dogs were anesthetized with intravenous thiamylal sodium and succinylcholine,

intubated, and mechanically ventilated. Under sterile conditions a thoracotomy was performed through the left fifth intercostal space. Silicone rubber pneumatic occluders were positioned around both venae cavae. A pericardiotomy was made from the apex of the heart to the great vessels and a silicone rubber tube (2.6 mm i.d., 4.9 mm o.d.) was placed into the left atrium through a purse-string suture in the base of the left atrial appendage for subsequent passage of a micromanometer across the mitral valve into the left ventricle (LV). A similar tube with multiple side holes was sutured to the epicardial surface of the base of the heart to allow measurement of pleural pressure. One pair of pulse transit ultrasonic dimension transducers [OL-84] oriented across the LV minor axis diameter was sutured to the epicardial surface of the LV. The catheters, transducer leads, and caval occluder tubes exited through the chest wall into a subcutaneous pouch dorsal to the thoracotomy incision. The pericardium was left widely open, and the thoracotomy was repaired in layers. Each dog was allowed to recover for seven to ten days before the hardware was exteriorized through a small skin incision. Though implanted, the vena caval occluders were not utilized in the present experiment.

One to three days after exteriorization of hardware, each dog was returned to the laboratory and a sedated state was induced and maintained by the titrated continuous infusion of thiamylal. A femoral vein and artery were

surgically isolated and cannulated with, respectively, a multilumen catheter for administration of the study drugs and a small plastic tube to facilitate measurement of arterial blood pressure. The tip of the multilumen catheter was advanced to a position just proximal to the right atrium.

The animals were studied while lying on their right side in the sedated state. They were allowed to ventilate spontaneously and responded to being petted or spoken to. The ultrasonic dimension transducers were coupled to a sonomicrometer. With this device, the time required for transmission of a burst of ultrasound from one of the piezoelectric transducers to the opposite transducer was measured and converted into an analog voltage output, which was linearly proportional to the distance between the transducers and therefore measured the length of the LV minor axis diameter. The minimum resolution of this system was approximately 0.08 mm and the maximum electronic drift was 0.05 mm/hr. High fidelity micromanometer-tipped catheters were passed through the implanted tubes into the LV and pleural space, and advanced through the femoral artery cannula into the ascending aorta. The micromanometers were prewarmed in a water bath at 38°C and were balanced and calibrated against a water column immediately before each study. Resultant manometer drift was less than 0.05 mm Hg per hour.

The experimental protocol nominally lasted for six hours and involved as many as four separate identification studies using PRB infusion of sodium nitroprusside and/or the  $\beta$ -adrenergic receptor antagonist esmolol [GO-85]. The results of these extensive experiments will be reported elsewhere, and only those details pertaining to identification of the hemodynamic response to nitroprusside will be discussed in this report.

The six dogs included in this discussion received PRB infusion of nitroprusside at rates switching between 1.0 and 0.0  $\mu\text{g}\cdot\text{kg}^{-1}\cdot\text{min}^{-1}$ . This was added to a continuous infusion of nitroprusside at 0.5  $\mu\text{g}\cdot\text{kg}^{-1}\cdot\text{min}^{-1}$ . Therefore, the PRB infusion of nitroprusside was effectively administered at amplitudes of  $\pm 0.5 \mu\text{g}\cdot\text{kg}^{-1}\cdot\text{min}^{-1}$  added to a continuous infusion of 1.0  $\mu\text{g}\cdot\text{kg}^{-1}\cdot\text{min}^{-1}$ . The purpose for the continuous infusion was to bias the system (canine hemodynamic response to nitroprusside) into its relatively linear operating range (in terms of the mean arterial blood pressure response) by infusing the nitroprusside at rates above a hypothetical initial shallow segment of its dose-response curve.

A 63-state maximum-length pseudo-random binary sequence of ones and zeros was generated to direct the nitroprusside infusion. A different sequence was generated for each dog by using various delayed versions of the original sequence [DA-70]. Each state was maintained for 29 seconds, giving a total PRB signal period length of 1827 seconds, well beyond

the system settling time. During 1-states nitroprusside was infused at the  $1.0 \mu\text{g}\cdot\text{kg}^{-1}\cdot\text{min}^{-1}$  rate and during 0-states at  $0.0 \mu\text{g}\cdot\text{kg}^{-1}\cdot\text{min}^{-1}$ . With 63 states of 29 seconds duration this PRB signal had an effective bandwidth of 0.000574 Hz ( $1/m\lambda$ ) to 0.011494 Hz ( $1/3\lambda$ ). Sheppard [SH-76] found that a 15-state PRB sequence length and a switching interval of 20 seconds (bandwidth of 0.003 Hz to 0.016 Hz) produced relatively reproducible nitroprusside impulse response curves in dogs and humans. The complete investigation was designed to acquire impulse response estimates by PRB testing with nitroprusside alone, esmolol alone, and from 2-input PRB testing with nitroprusside and esmolol. The sequence length and switching interval selected for the study were a compromise between the desire to identify a fast-acting system (nitroprusside; requiring a brief switching interval), a relatively slow-acting system (esmolol, with an elimination half-life of 9 minutes [QU-86]; requiring a long sequence length and switching interval), and the constraints of multidimensional PRB testing [DA-70].

A software program operating on a microcomputer was used to implement the PRB infusion of nitroprusside by controlling a peristaltic drug infusion pump. Distortion of the PRB pharmacological input perturbation due to the mechanics of the infusion system was considered to be negligible.

Hemodynamic data included in this report were collected during the second period of two consecutive contiguous

repetitions of the PRB nitroprusside infusion. During this second period, analog voltages representing LV pressure, pleural pressure, arterial pressure, LV minor axis segment length, and the activity of the infusion pump were digitized at 200 samples per second by a computerized data acquisition system and stored on digital magnetic tape for subsequent analysis. The excessive duration of the PRB infusion period in the context of the other PRB interventions that were performed during these experiments and concern for stability of the animal preparation precluded data collection from additional repetitions of the infusion sequence.

### 3.2 Methods - Data Analysis

Data analysis was performed in two stages. The result of the first stage was creation of files containing beat-to-beat measured and derived hemodynamic data. During the second stage of data reduction the crosscorrelation and subsequent analyses pertaining to PRB testing were performed.

The first stage of data analysis was performed on a minicomputer using previously developed [GL-85] software. LV transmural pressure was calculated as LV pressure minus pleural pressure; for the remainder of this report, all references to ventricular pressures are transmural pressures. The time derivative of LV pressure,  $dp/dt$ , was computed from the digital pressure waveform as a running five-point polyorthogonal transformation. Beginning- and end-ejection and beginning- and end-diastole of each cardiac

cycle were defined by the computer [GL-85]. Beatpoint definitions were checked visually by the investigator on all data with an interactive videographics display system and were manually redefined when necessary. For the purposes of the data included in this report, approximately 26,000 cardiac cycles were thus analyzed.

Cardiac cycles were defined as the interval from beginning-diastole to beginning-diastole. On a beat-to-beat basis, numerical files containing the following data were created: beatpoint number at beginning-diastole, heart rate (HR), end-diastolic LV pressure (EDP) and minor axis diameter (EDL), mean LV ejection pressure (MEP), LV minor axis ejection shortening (EJS), peak positive (DPP) and peak negative (DPN)  $dp/dt$ , mean arterial blood pressure (MAP), diastolic arterial pressure (DAP), systolic arterial pressure (SAP), stroke work (SW), and a voltage level (high/low) indicating the status of the drug infusion pump (on/off, respectively).

The beatpoint number referenced the data sample number (in 5 millisecond intervals) at the time of beginning diastole, thereby allowing each cardiac cycle to be referenced in absolute time. Heart rate was defined as the reciprocal of the duration (minutes) of the cardiac cycle. Mean LV ejection pressure was defined as the average LV pressure during the ejection phase of the cardiac cycle. Similarly, ejection shortening was defined as the difference between the minor axis diameter at end- and beginning-

ejection. Systolic and diastolic pressures were defined as the maximum and minimum values, respectively, of the arterial pressure waveform over the cardiac cycle, and mean arterial pressure was the arithmetic average of the digitized arterial pressure waveform over the cardiac cycle. Stroke work was defined as the area within each LV pressure-diameter loop. Insomuch as LV volume was not measured or computed, this was not true stroke work, but it has been demonstrated that LV minor axis diameter is linearly related to ventricular volume under most conditions [SU-74]. Therefore, the calculation of stroke work used in this study should be directly proportional to stroke work defined as the integral of LV pressure with respect to volume. The drug infusion pump status was transformed to  $+0.5$  ( $\mu\text{g}\cdot\text{kg}^{-1}\cdot\text{min}^{-1}$ ) for pump on and  $-0.5$  ( $\mu\text{g}\cdot\text{kg}^{-1}\cdot\text{min}^{-1}$ ) for pump off for each cardiac cycle, with the  $+0.5$  level being used whenever the pump changed states during the cardiac cycle.

These numerical data files were "sampled" at evenly spaced 1 second intervals by collecting into new files the data from the cardiac cycle occurring at the time of each of the 1827 seconds during the data collection period. All subsequent analyses were performed using these sampled-data files.

In the second stage of data analysis, these derived data files were analyzed for the purpose of comparing the utility of the impulse response estimates obtained by crosscorrelation versus the best approximate impulse

response estimate and for using these impulse response estimates to learn more about the pharmacodynamics of nitroprusside. These analyses were performed using a microcomputer with software programs written in Fortran. Unless otherwise stated, these programs were written by the investigator. All floating point and transcendental calculations were performed in double precision arithmetic supported by an 8087 math coprocessor.

Linear regression analysis was used to determine the y-intercept and slope of each data sequence. The arithmetic average of each hemodynamic data file was calculated and then subtracted from each element in the data sequence. The crosscorrelation sequence for each zero-mean hemodynamic data file and its respective sampled PRB sequence was computed according to equation (2-3-2). These crosscorrelations were scaled (see equation 2-3-9) by dividing each element by 0.25 ( $=\alpha^2$ ) and normalized according to property 5 in Section 2.2 by dividing each element by 29 ( $=s$ ). All subsequent references to the crosscorrelation sequence will be understood to mean a sequence that has been scaled and, unless stated otherwise, normalized.

The autocorrelation sequence for one of the sampled PRB sequences was computed according to equation (2-2-1). Since all of the PRB sequences used to infuse nitroprusside were merely circularly shifted versions of each other, their autocorrelation sequences were identical. The generalized inverse of the 1827x1827 autocorrelation matrix ( $\Phi_{xx}$ ) was

obtained by computing the inverse discrete Fourier transform of the autocorrelation sequence, invoking the transformation of equation (2-4-2), and then computing the forward discrete Fourier transform. Double precision implementations of the algorithms of Monro [MO-73] were used to compute the Fourier transformations (see Appendix A). According to equation (2-4-5), the unscaled and non-normalized crosscorrelation sequences were multiplied by the generalized inverse of the autocorrelation matrix to obtain the best approximate impulse response sequence estimate.

For each of the eleven hemodynamic variables studied, the arithmetic average at each point of the first 512 points (8.53 minutes) of the six (six dogs) time-shifted crosscorrelations was determined. These average values then defined the mean crosscorrelation impulse response curve. It was known from previous studies [SH-76, 82] that the effects of nitroprusside last for only three to five minutes. Therefore, eight minutes were more than adequate to capture the interesting portion of the impulse response curves and 512 data points (512 seconds of data) were utilized for the sake of convenience in performing the subsequent discrete Fourier transforms.

For each variable the following equation [BE-79, SH-76] was used to compute the correlation between the mean crosscorrelation curve and each of the six individual crosscorrelation impulse response curves:

$$r_k = \frac{\frac{1}{2} \sum_{p=1}^P (\langle\langle c_p \rangle\rangle c_{kp} + \langle\langle s_p \rangle\rangle s_{kp})}{\left( \frac{1}{2} \sum_{p=1}^P (\langle\langle c_p \rangle\rangle^2 + \langle\langle s_p \rangle\rangle^2) \cdot \frac{1}{2} \sum_{p=1}^P (c_{kp}^2 + s_{kp}^2) \right)^{1/2}} \quad (3-2-1)$$

where:

- $r_k$  = correlation of the k-th impulse response with the average
- $k$  = impulse response number
- $p$  = harmonic number
- $c_{kp}$  = cosine coefficient for k-th impulse response and p-th harmonic
- $s_{kp}$  = sine coefficient for k-th impulse response and p-th harmonic
- $\langle\langle c_p \rangle\rangle$  = cosine coefficient for p-th harmonic of the average impulse response
- $\langle\langle s_p \rangle\rangle$  = sine coefficient for p-th harmonic of the average impulse response
- $P$  = total number of harmonics.

In the present application,  $k$  ranged from 1 to 6 and  $P$  was 256. The Fourier coefficients were computed using a double precision implementation of the fast Fourier transform algorithm FASTF [MO-73]. These procedures were also performed using the time-shifted best approximate impulse responses.

Each of the crosscorrelation impulse response estimates were convolved twice contiguously with the sampled PRBS

sequence from which it was derived. The mean-square error between the sequence resulting from the second period of this convolution and the zero-mean sequence of hemodynamic data used to derive the particular impulse response estimate was calculated. To compute the mean-square error [MA-78], the sum of the squares of the zero-mean hemodynamic data sequence was calculated and normalized to a value of 100. Then, the sum of the squares of the difference between the convolution sequence and the data sequence was multiplied by the normalization factor just determined and this value was defined as the mean-square error between the two sequences. These convolution and subsequent procedures were repeated with the best approximate impulse response estimates, and with low-pass filtered versions of the two types of impulse response estimates. Low-pass filtering with a cutoff frequency of 0.011494252 Hz ( $=1/3\lambda$ ) was performed using a double-precision implementation of the phaseless 3-rd order digital Butterworth filtering algorithm of Pynsent and Hanka [PY-82].

Impulse response estimates reflecting the baroreceptor reflex control of heart rate were analyzed as an example of the utility of these discrete waveforms to provide conventional physiological information. Visual inspection of the time-shifted crosscorrelation impulse response estimates for heart rate and mean arterial blood pressure suggested that the dynamic portion of these curves were relatively linear in the intervals from 28 to 51 seconds

(activation period) and 75 to 102 seconds (deactivation period). Linear regression analysis was used to obtain the x-axis (time) intercept for the heart rate and mean arterial pressure impulse response sequences during these intervals; this was done using the time-shifted, crosscorrelation impulse response estimates, filtered as before and unfiltered, and the filtered best approximate impulse response estimate. The difference between the pressure x-intercept and the heart rate x-intercept for both intervals was calculated as an estimate of the time lag between the pressure response and the heart rate response. For the same time intervals and same impulse response sequences, linear regression with the pressure response as the independent variable and the heart rate response as the dependent variable yielded a slope that was used as an estimate of the closed-loop gain of the baroreflex heart rate control system.

As the final step in data analysis, a simulation of closed-loop infusion of nitroprusside was devised. A software program (see Appendix B) implementing Sheppard's [SH-76, 80, RE-78] closed-loop infusion algorithm for nitroprusside was written which incorporated a routine to perform numerical convolution of the infusion rates output by the algorithm with the time-shifted best approximate impulse response estimate for mean arterial blood pressure from one dog (dog 1) to provide the simulated feedback signal when summed with the previously determined mean value of the

original hemodynamic data sequence. The nitroprusside infusion rates ( $\mu\text{g}\cdot\text{kg}^{-1}\cdot\text{min}^{-1}$ ) specified by the control algorithm during the simulation were collected into a data file, which was subsequently convolved with the ten other best approximate impulse response estimates from the same dog to simulate (when summed with the mean value of each respective original data sequence) a complete hemodynamic profile during the closed-loop nitroprusside infusion.

Comparative statistics were deemed inappropriate in consideration of the small sample size ( $n=6$ ). Data are expressed as mean $\pm$ S.D.

## CHAPTER 4

### RESULTS

The means of the average value of each hemodynamic data sequence, as well as the slope and y-intercept of the data sequence, are given in table 4-1. There was excellent agreement between the arithmetic means of the sequences and the y-intercepts determined by linear regression analysis, and the slopes of the regression lines were generally negligible; these data demonstrate the relative stability of the animal preparation. The heart rate and arterial and mean LV ejection pressures profile of one dog (dog 5) during PRB infusion of nitroprusside is shown in figure 4-1. The PRB infusion sequence used to generate these data is also included in this figure. Demonstrated is the hypotensive effect of nitroprusside and an inverse relationship between blood pressure and heart rate.

The non-normalized crosscorrelation between the zero-mean mean arterial blood pressure response of one dog (dog 1) and its respective sampled PRB infusion signal is shown in figure 4-2. The scaled and normalized time-shifted version of this crosscorrelation sequence is shown in figure 4-3 and demonstrates the intuitively pleasing effect of

Table 4-1. Means and linear regression parameters for sampled hemodynamic data sequences. Units are given for the mean and y-intercept. Slope is in units of  $\Delta\text{unit} \cdot \Delta\text{minute}^{-1}$ .

	SEQUENCE MEAN	Y-INTERCEPT	SLOPE
DAP (mm Hg)	71.4±12.1	73.0±12.9	-0.02±0.08
DPN (mm Hg/sec)	-1344±210	-1370±227	1.68±2.66
DPP (mm Hg/sec)	1307±248	1312±239	-0.358±2.61
EDL (mm)	56.2±4.4	56.3±4.4	-5.0E-3±0.012
EDP (mm Hg)	10.35±1.74	10.44±2.11	-6.0E-3±0.040
EJS (mm)	2.30±0.54	2.29±0.57	4.0E-4±3E-3
HR (bpm)	136±19	135±22	0.07±0.35
MAP (mm Hg)	79.9±10.9	81.8±11.9	-0.12±0.25
MEP (mm Hg)	73.3±6.7	74.6±6.6	-0.08±0.15
SAP (mm Hg)	93.0±9.9	94.4±10.8	-0.09±0.20
SW (N/mm)	0.0187±0.0042	0.0189±0.0045	-1.4E-5±5.E-4

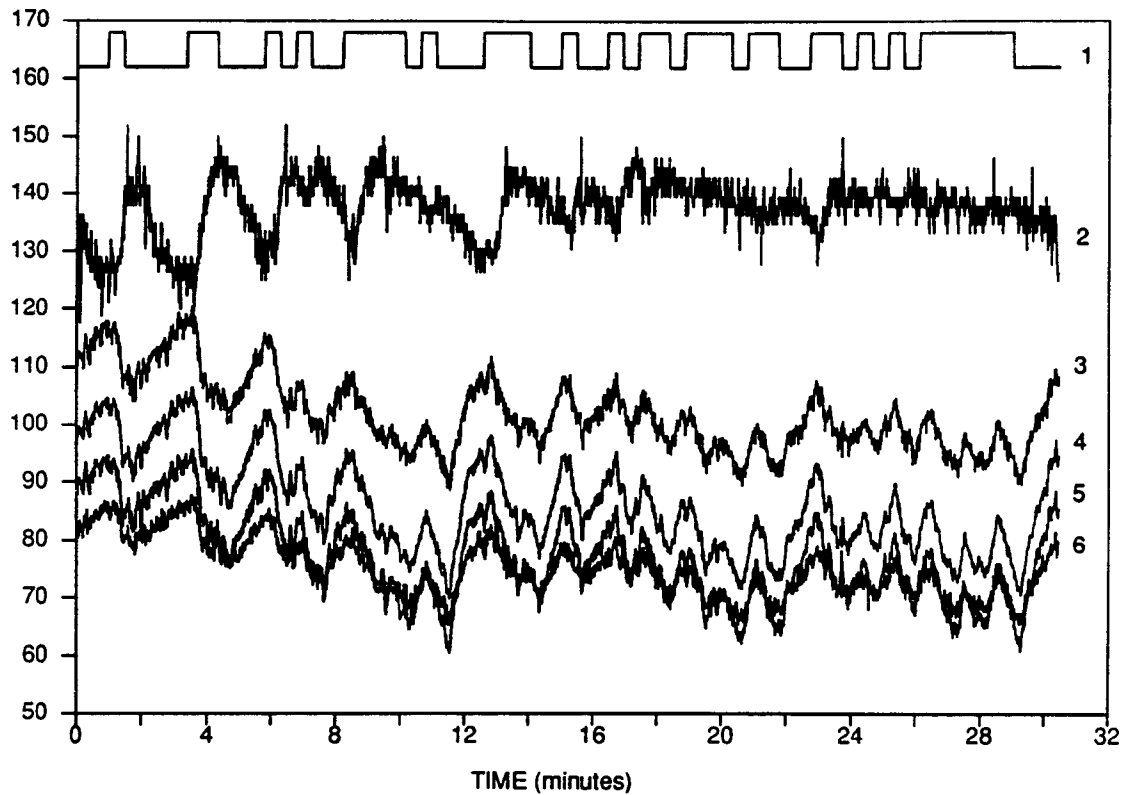


Figure 4-1. Blood pressure and heart rate data from one dog during PRB nitroprusside infusion. Legend: 1-schematic representation of nitroprusside infusion signal; 2-heart rate; 3-systolic, 4-mean, 5-diastolic arterial pressure; 6-mean LV ejection pressure. Units: 1-high=pump on, low=pump off; 2-bpm; 3 through 6-mm Hg.

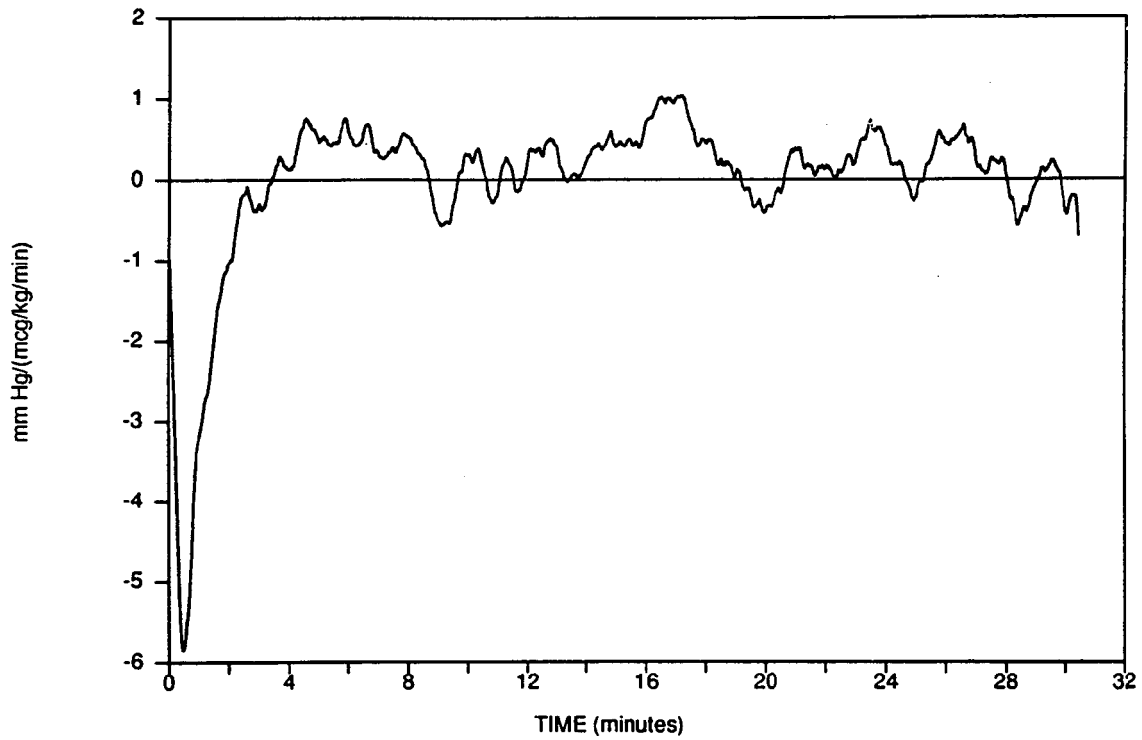


Figure 4-2. Non-normalized crosscorrelation estimate. Example from one dog for mean arterial pressure.

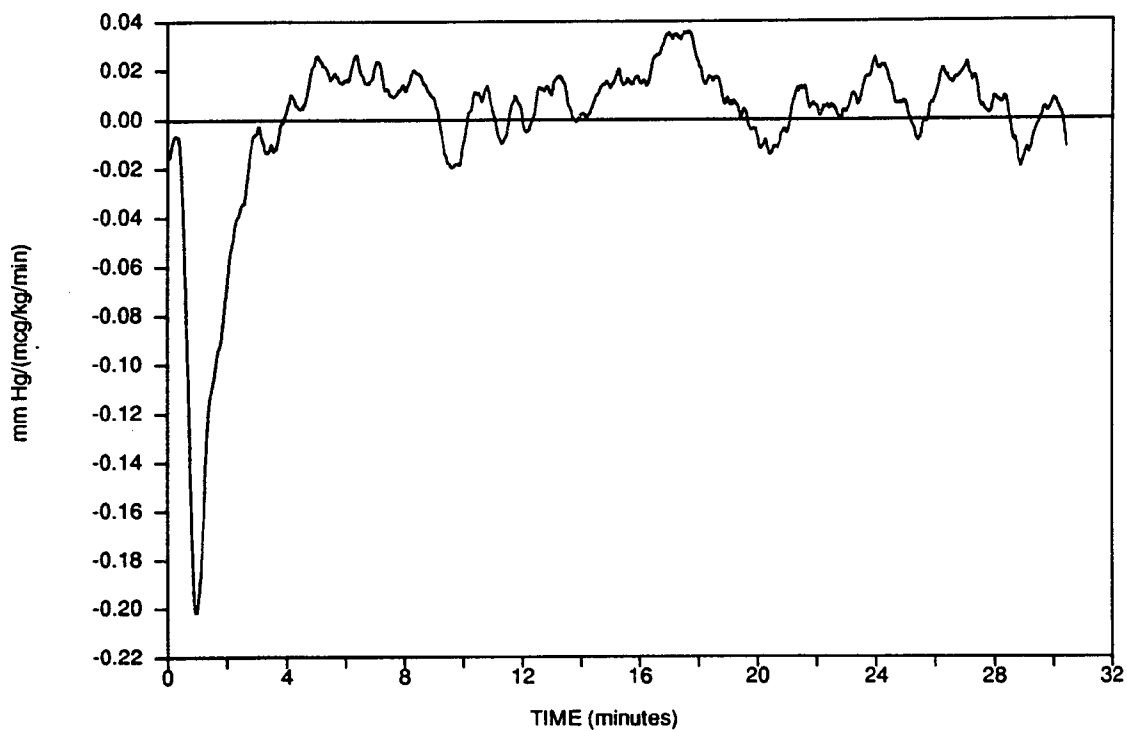


Figure 4-3. Normalized, time-shifted crosscorrelation estimate. Example from one dog for mean arterial blood pressure.

time-shifting the impulse response estimate. All units labels of  $\mu\text{g}\cdot\text{kg}^{-1}\cdot\text{min}^{-1}$  are nitroprusside infusion rates.

Shown in figures 4-4 through 4-7 are the first 512 points in the mean time-shifted crosscorrelation impulse response estimate sequences for each of the eleven hemodynamic parameters studied. Figure 4-4 again demonstrates the inverse relationship between heart rate and systemic blood pressure. The impulse response estimates for mean and diastolic pressures were virtually identical and were of greater magnitude than the systolic arterial pressure response, and all three systemic pressure variables showed a greater change than mean LV ejection pressure. All of these curves are characterized by a pure time delay of about 0.37 minutes and a time to apex (heart rate) or nadir (pressures) of about 1.1 minutes. These impulse responses decayed to baseline by about 2.6 minutes. The mean impulse response estimates for end-diastolic LV pressure and minor axis diameter (figure 4-5) were similar in shape to those of the arterial pressures, but were somewhat more prolonged. Peak positive LV  $dP/dt$  (figure 4-6) showed little if any response to nitroprusside, but peak negative  $dP/dt$  demonstrated a distinct increase, with a time-course similar to, though slightly more prolonged than, the heart rate response. Ejection shortening (figure 4-7) also responded in a manner similar to heart rate, whereas LV stroke work declined slightly and demonstrated a prolonged recovery to baseline. Correlation analysis of these mean

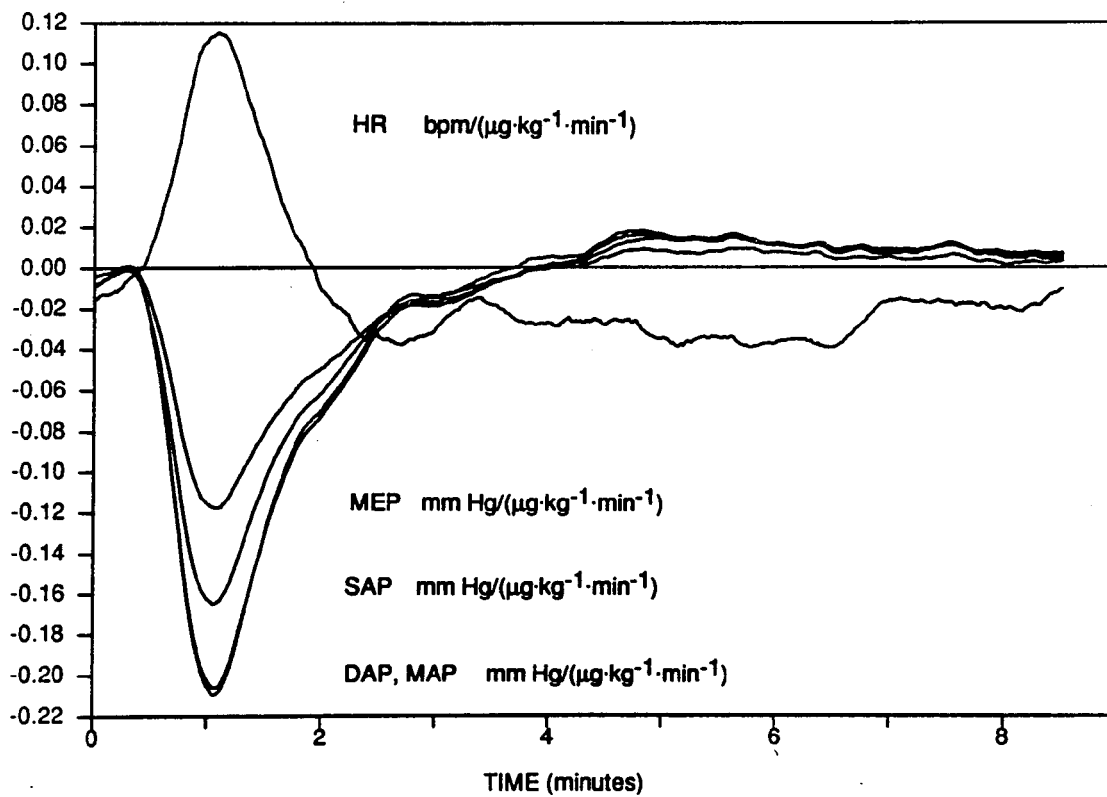


Figure 4-4. Average normalized crosscorrelation estimates for heart rate and LV ejection and arterial pressures.

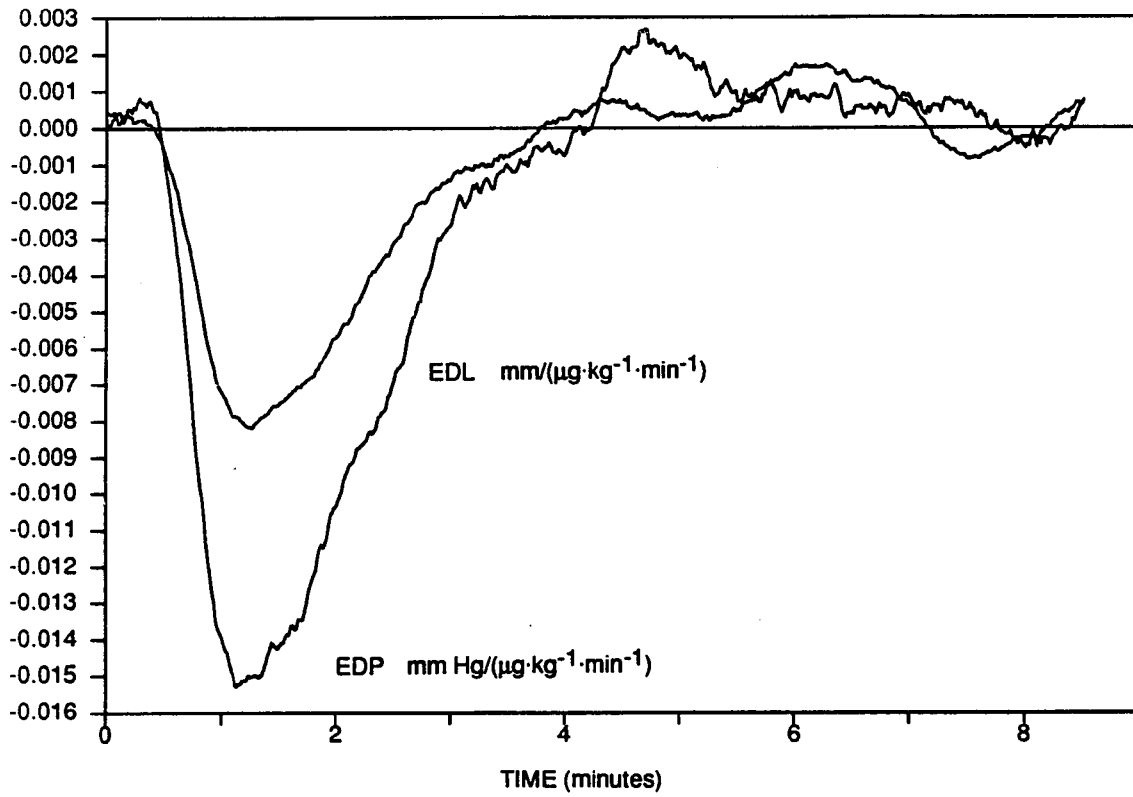


Figure 4-5. Average normalized crosscorrelation estimates for end-diastolic pressure and minor axis diameter.

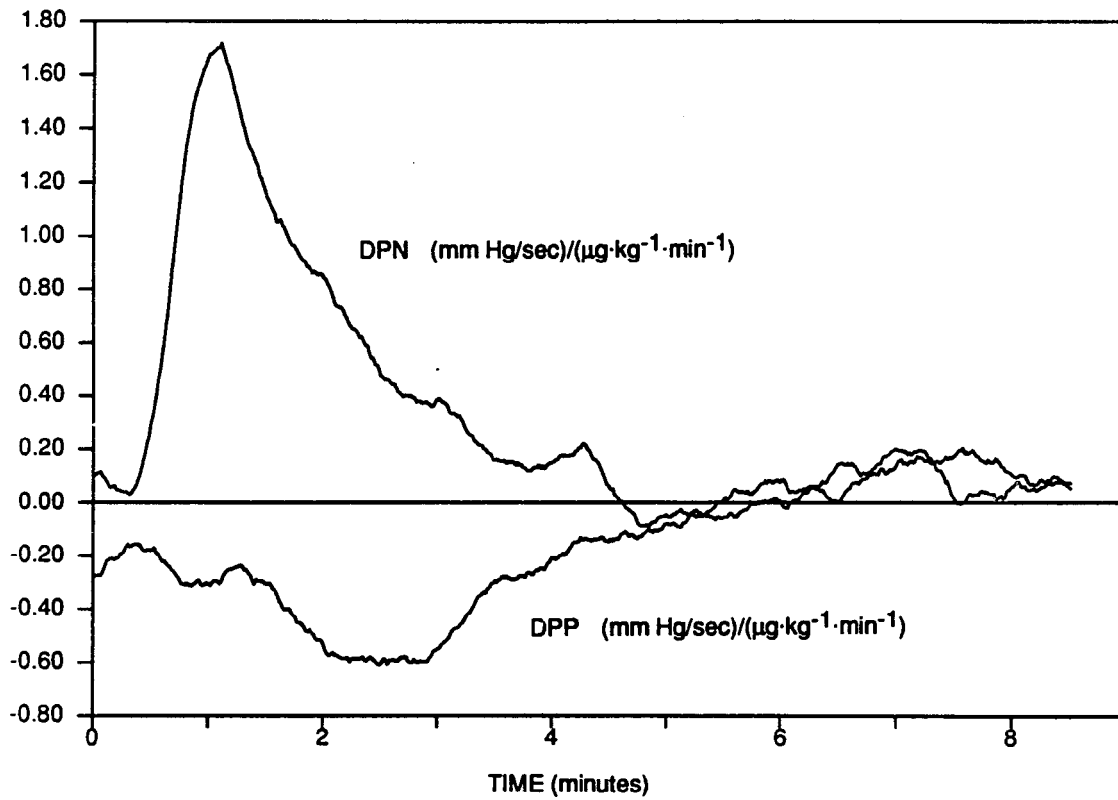


Figure 4-6. Average normalized crosscorrelation estimates for positive and negative LV  $dp/dt$ .

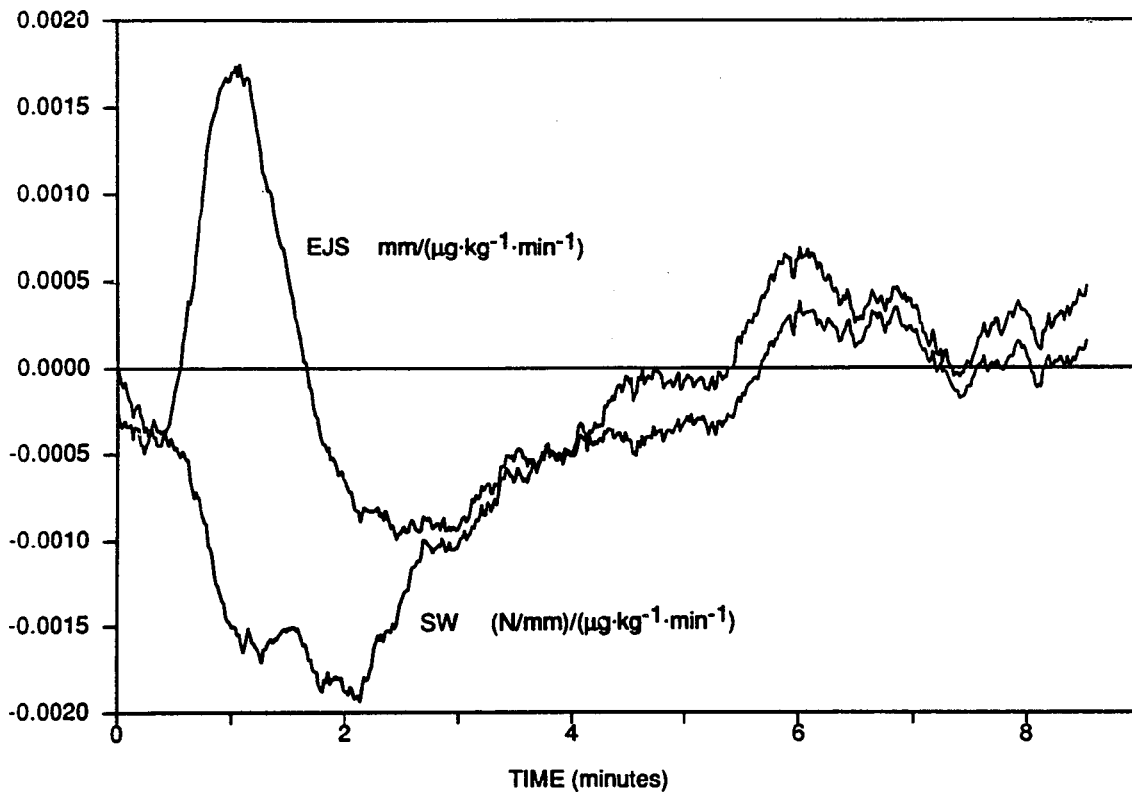


Figure 4-7. Average normalized crosscorrelation estimates for ejection shortening and stroke work. Stroke work estimate was multiplied by 100 for convenience in plotting.

crosscorrelation impulse response curves with each of the individual response sequences is summarized in table 4-2. With few exceptions (e.g., peak positive LV dP/dt for dog 3), the individual crosscorrelation estimates were well represented by the average curves, most of the regression coefficients (equation 3-2-1) being greater than 0.85. The impulse response estimates for ejection shortening were less well characterized by their average than were most of the other variables. In general, sequences from dogs 3 and 4 had lower regression coefficients than did those of the other dogs. There was no correlation between the average best approximate impulse responses and each of the individual best approximate estimates (table 4-3).

As an example of the amplitude distortion manifested in convolution with the sampled PRB testing-derived impulse response estimates, figure 4-8 shows the sequence resulting from convolution of a non-normalized crosscorrelation impulse response estimate (figure 4-2) for mean arterial blood pressure with its respective PRB sequence. The dynamic range of the waveform in this figure is approximately  $\pm 200$  mm Hg, an order of magnitude greater (exactly 29 times greater) than the response to nitroprusside observed in the animal experiment. Convolution using the normalized crosscorrelation model yielded the waveform in figure 4-9, which is different than the raw data sequence by a mean-square error equivalent to

Table 4-2. Correlation between the average cross-correlation impulse response estimate and each individual estimate for each variable

CORRELATION COEFFICIENT							
DOG:	1	2	3	4	5	6	Mean±S.D.
DAP	.9843	.9773	.8432	.9198	.9812	.9855	.9485±.0574
DPN	.9390	.9656	.3864	.8434	.9599	.8134	.8180±.2207
DPP	.9058	.8281	.0228	.3912	.9702	.9531	.6785±.3865
EDL	.9424	.9566	.8500	.0144	.9644	.9398	.7779±.3763
EDP	.9309	.8973	.8619	.6712	.9666	.9380	.8777±.1074
EJS	.7186	.8283	.6772	.8635	.7830	.4249	.7159±.1582
HR	.9738	.7658	.9694	.8379	.9729	.9753	.9158±.0912
MAP	.9877	.9805	.8332	.9160	.9829	.9872	.9479±.0626
MEP	.9881	.9784	.7799	.9097	.9820	.9900	.9380±.0832
SAP	.9918	.9806	.8194	.9111	.9802	.9883	.9452±.0686
SW	.8670	.9289	.0051	.7091	.9311	.9187	.7266±.3634
Mean	.9299	.9170	.6408	.7261	.9522	.9013	
±S.D.	.0805	.0765	.3438	.2844	.0580	.1661	

Table 4-3. Correlation between the average best approximate impulse response estimate and each individual best approximate estimate for each variable

CORRELATION COEFFICIENT							
DOG:	1	2	3	4	5	6	Mean±S.D.
DAP	.3872	.3396	.5152	.4750	.1549	.5330	.4008±.1418
DPN	.3966	.4745	.4088	.2682	.3963	.4170	.3936±.0679
DPP	.4277	.5241	.3872	.3768	.4054	.2923	.4022±.0755
EDL	.0536	.3766	.2969	.6251	.2755	.5628	.3651±.2081
EDP	.3414	.3006	.6498	.3590	.4313	.4551	.4229±.1251
EJS	.2517	.2718	.4775	.5736	.1853	.3741	.3557±.1480
HR	.1997	.6516	.4802	.5060	.3050	.1860	.3881±.1871
MAP	.3477	.1500	.3420	.5962	.3417	.5189	.3827±.1567
MEP	.0239	.4017	.5759	.5131	.3346	.1747	.3373±.2082
SAP	.4160	.1551	.3895	.6483	.3524	.4504	.4019±.1592
SW	.3592	.3680	.4151	.4328	.2800	.4742	.3882±.0679
Mean	.2913	.3649	.4489	.4886	.3148	.4035	
±S.D.	.1424	.1499	.1039	.1204	.0873	.1336	

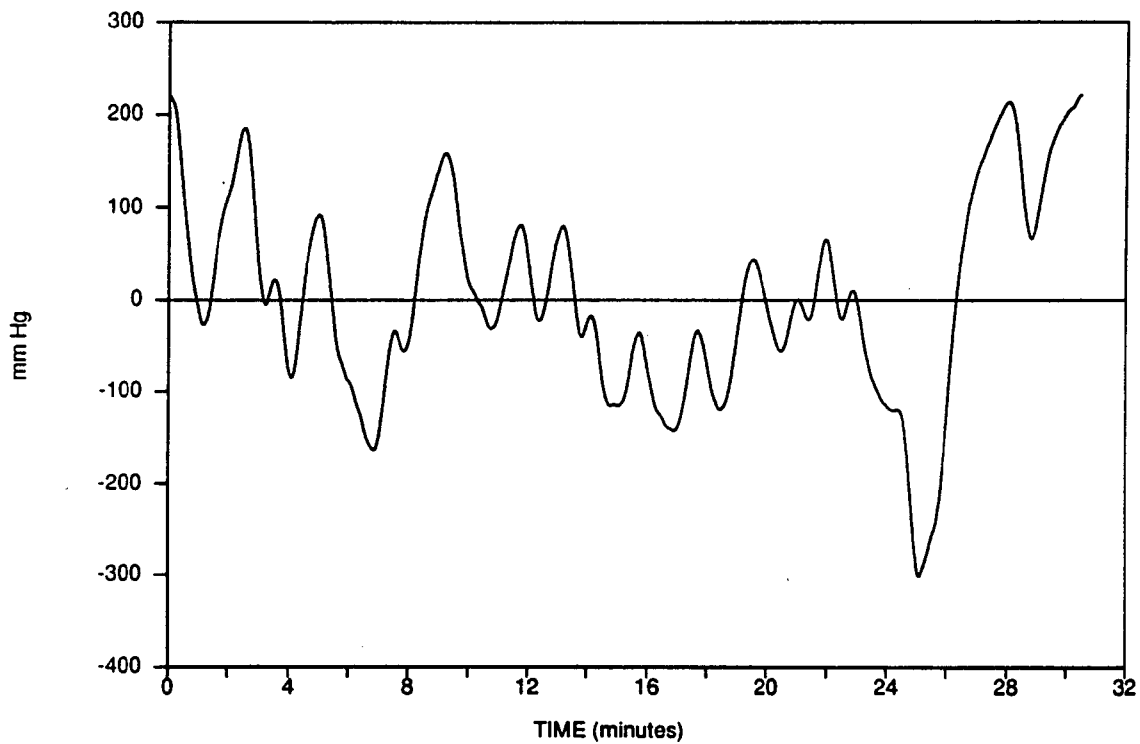


Figure 4-8. Convolution with non-normalized crosscorrelation. Line represents convolution estimate for mean arterial pressure from one dog.

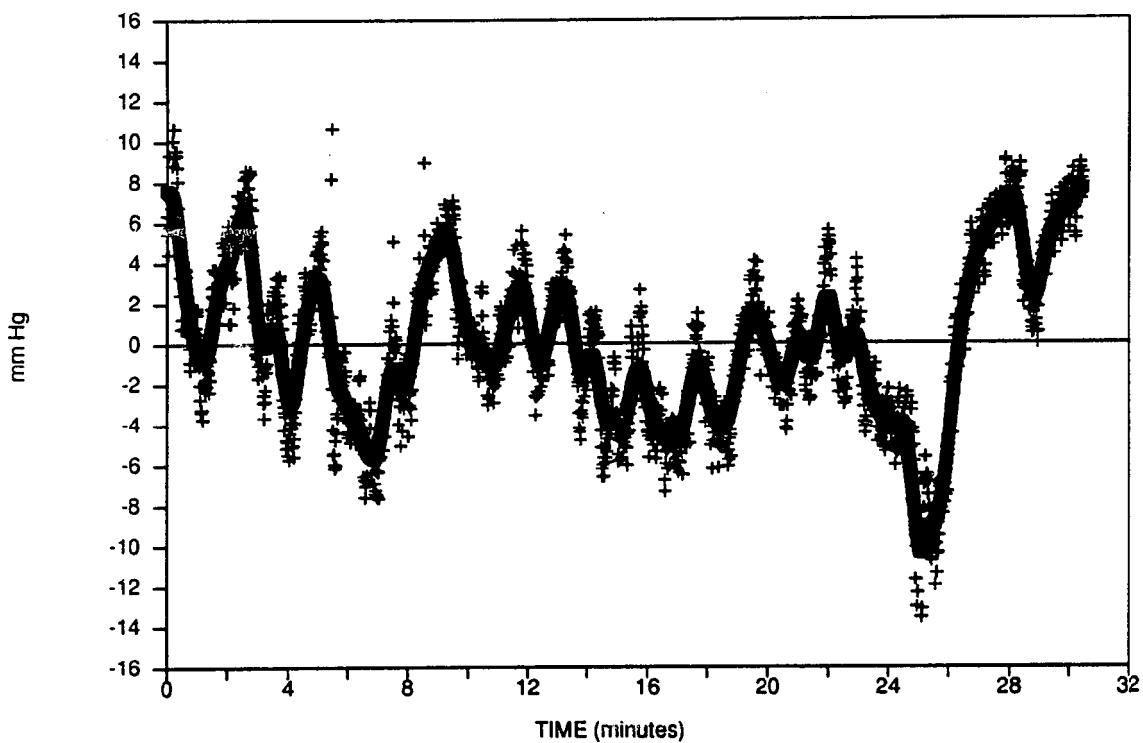


Figure 4-9. Convolution with normalized crosscorrelation. Example from one dog for mean arterial pressure. Crosses represent actual data during PRB nitroprusside infusion. Solid line represents convolution of the PRB sequence with the normalized crosscorrelation impulse response estimate (cf. figure 4-8).

2.21 mm Hg<sup>2</sup>. The model sequences in figures 4-8 and 4-9 are different only by a multiplicative scale factor ( $= s = 29$ ).

The sequence of the first row (or column) elements of the circulant generalized inverse of the 1827x1827 autocorrelation matrix for the sampled PRB signal used in this study is shown as a line spectrum in figure 4-10. The time-shifted best approximate impulse response estimate for mean arterial blood pressure for one dog (dog 1) is shown in figure 4-11 (cf. figure 4-3). Convolution of this best approximate model (non-time-shifted) with its respective PRB sequence resulted in the sequence in figure 4-12, which is different than the raw data sequence (also shown for comparison) by an equivalent mean-square error of 0.04 mm Hg<sup>2</sup>. The relationship between the best approximate and crosscorrelation models is exemplified in figure 4-13 where the sequence from figure 4-3 and a filtered version of the sequence in figure 4-11 are plotted on the same set of axes.

Average mean-square errors for the sequences resulting from convolution with the various impulse response estimates are given in table 4-4. For each of the eleven hemodynamic variables studied, the mean-square errors resulting from best approximate impulse response models were generally less than 1.0 except for ejection shortening and stroke work. Filtered versions of the best approximate and crosscorrelation estimates produced sequences with mean-square errors that were relatively high, very similar, and

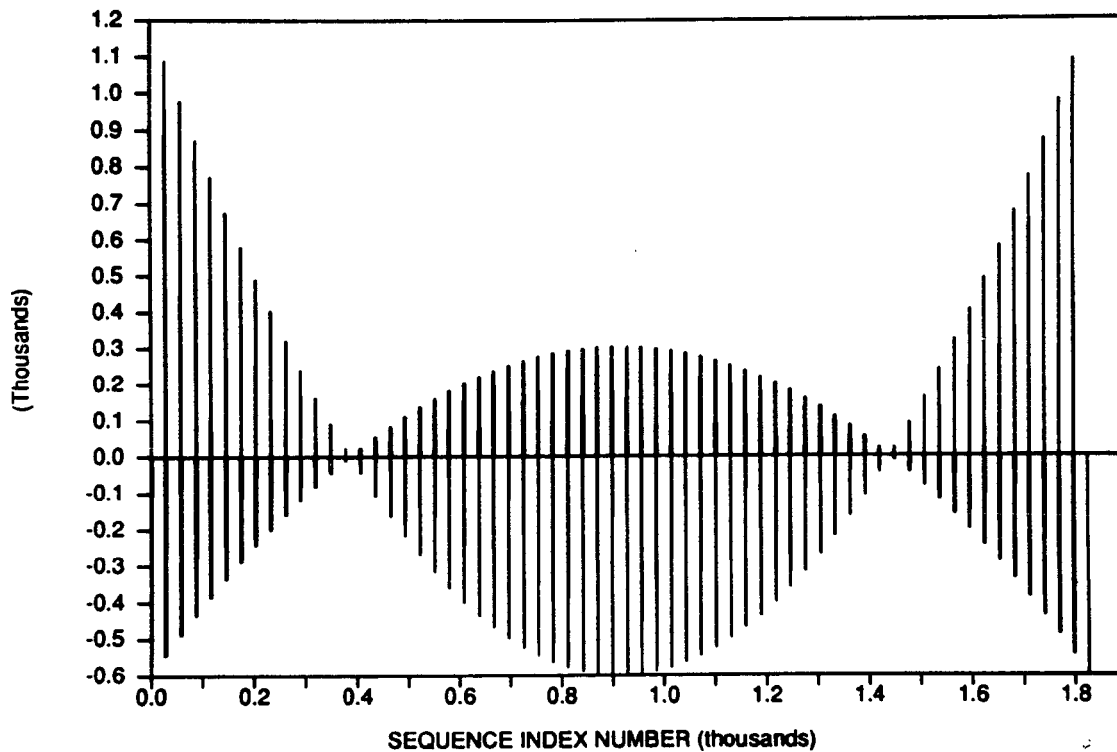


Figure 4-10. First row of generalized inverse of autocorrelation matrix. The generalized inverse of the autocorrelation matrix for the PRB sequence used in this study was an  $1827 \times 1827$  circulant matrix.

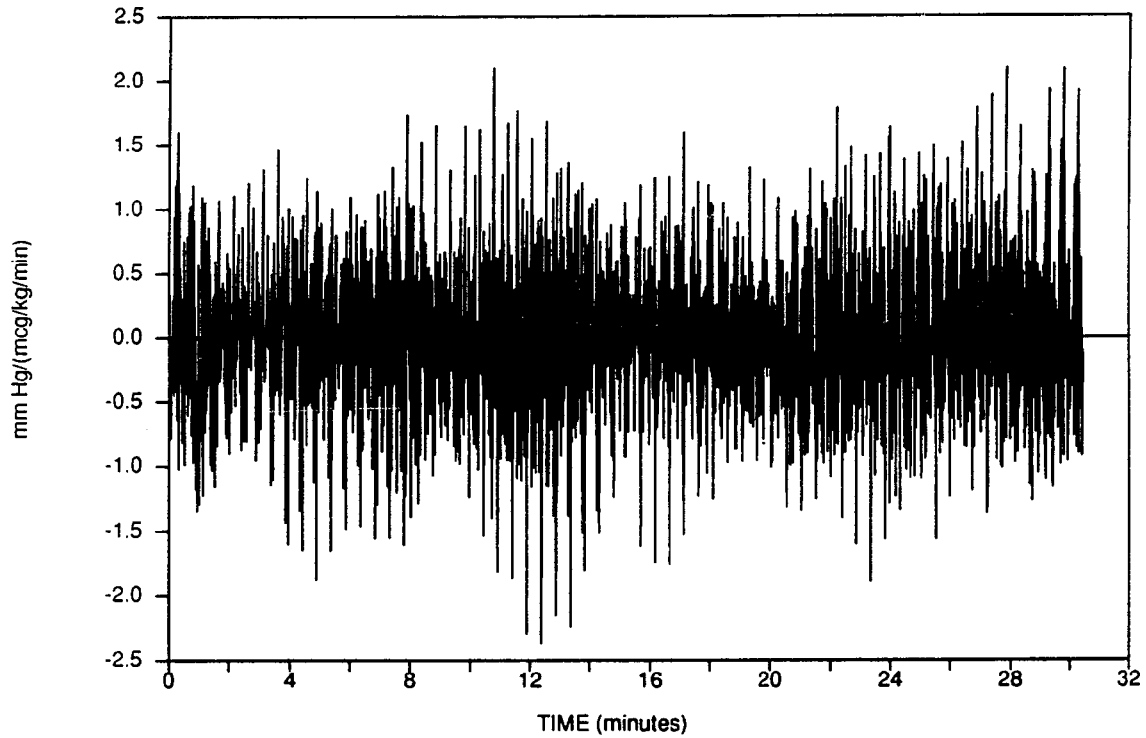


Figure 4-11. Best approximate impulse response estimate. Time-shifted example from one dog for mean arterial pressure (cf. figure 4-3).

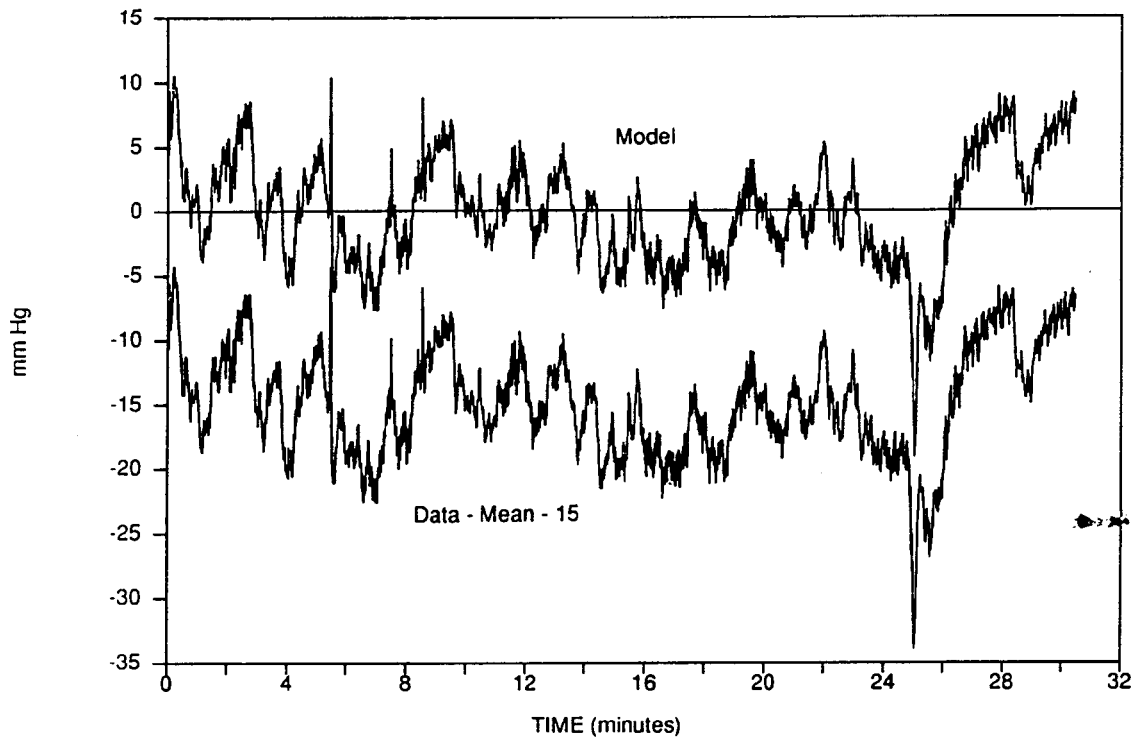


Figure 4-12. Convolution with best approximate impulse response. The model tracing is an example from one dog of convolution of the PRB sequence with the best approximate impulse response estimate for mean arterial pressure. Shown below it for reference (amplitude-shifted for clarity) is the actual data sequence.

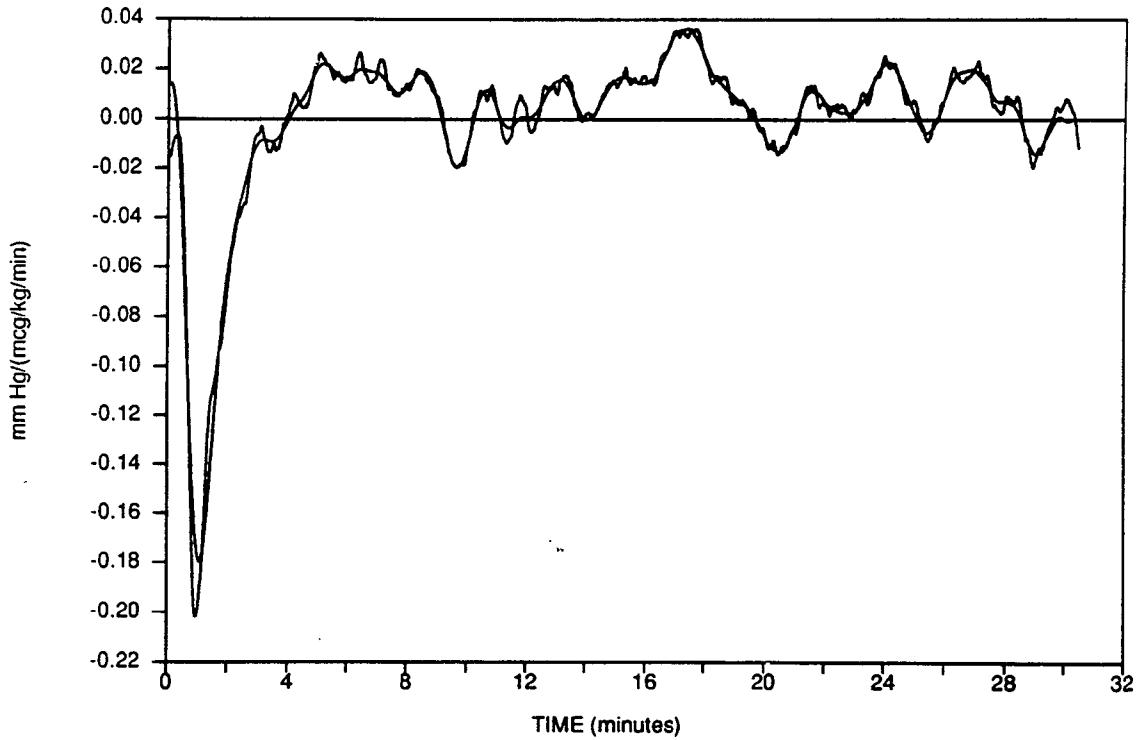


Figure 4-13. Comparison of normalized crosscorrelation and filtered best approximate impulse response estimate. Example from mean arterial pressure in one dog. Both sequences are time-shifted. The best approximate estimate is the smoother curve with a positive y-intercept.

Table 4-4. Mean-square errors between data sequences and model sequences. Averages are mean $\pm$ S.D., n=6. Model sequences for each dog for each variable were computed by convolving each of the impulse response types with its corresponding sampled PRB signal.

	MEAN-SQUARE ERRORS			
	NORMALIZED CROSSCORRELATION		BEST APPROXIMATE SOLUTION	
	FILTERED		FILTERED	
DAP	15.54 $\pm$ 7.38	21.37 $\pm$ 8.15	0.20 $\pm$ 0.12	19.64 $\pm$ 8.19
DPN	49.13 $\pm$ 15.19	53.38 $\pm$ 15.59	0.64 $\pm$ 0.28	51.11 $\pm$ 15.97
DPP	63.40 $\pm$ 16.59	66.66 $\pm$ 16.27	0.92 $\pm$ 0.28	66.65 $\pm$ 15.99
EDL	46.71 $\pm$ 19.72	49.93 $\pm$ 19.64	0.62 $\pm$ 0.38	49.73 $\pm$ 20.09
EDP	59.79 $\pm$ 20.81	62.50 $\pm$ 21.05	0.74 $\pm$ 0.35	62.46 $\pm$ 21.33
EJS	82.62 $\pm$ 8.44	85.70 $\pm$ 8.10	1.22 $\pm$ 0.30	87.73 $\pm$ 10.45
HR	38.38 $\pm$ 15.24	42.67 $\pm$ 14.98	0.63 $\pm$ 0.19	42.37 $\pm$ 14.66
MAP	13.37 $\pm$ 6.53	18.94 $\pm$ 7.61	0.17 $\pm$ 0.09	17.22 $\pm$ 7.46
MEP	21.75 $\pm$ 12.33	26.44 $\pm$ 13.14	0.31 $\pm$ 0.24	24.82 $\pm$ 12.96
SAP	20.51 $\pm$ 11.84	25.51 $\pm$ 12.64	0.24 $\pm$ 0.17	24.20 $\pm$ 12.40
SW	79.76 $\pm$ 8.51	82.30 $\pm$ 8.70	1.16 $\pm$ 0.40	83.23 $\pm$ 8.43

in every case higher than that achieved by convolution with the unfiltered crosscorrelation estimate.

Examples demonstrating use of the heart rate and mean arterial pressure impulse response sequences to calculate the response time and gain of the baroreceptor reflex system for heart rate control are shown in figures 4-14 and 4-15, respectively. Tabulated in table 4-5 for each dog are the activation and deactivation response times and gains determined from the crosscorrelation, filtered crosscorrelation, and filtered best approximate impulse response estimates. The activation response times were generally negative (heart rate response lagged behind blood pressure response) and the deactivation response times were generally positive (blood pressure response lagged behind heart rate response). Likewise, the activation gains were generally smaller than the deactivation gains. Although the correlation coefficients from the linear regression analyses used to obtain the results in table 4-5 averaged  $0.9881 \pm 0.0341$  ( $n=108$ ), there was a great deal of variability, even to the point of differences in sign, in the results computed among the six dogs and between the impulse response types.

Results of the simulation of closed-loop infusion of nitroprusside are given in figures 4-16 through 4-20. Systolic, diastolic, and mean arterial blood pressures and mean LV ejection (not shown) pressures all fell in parallel. The nitroprusside infusion rates generated by the control

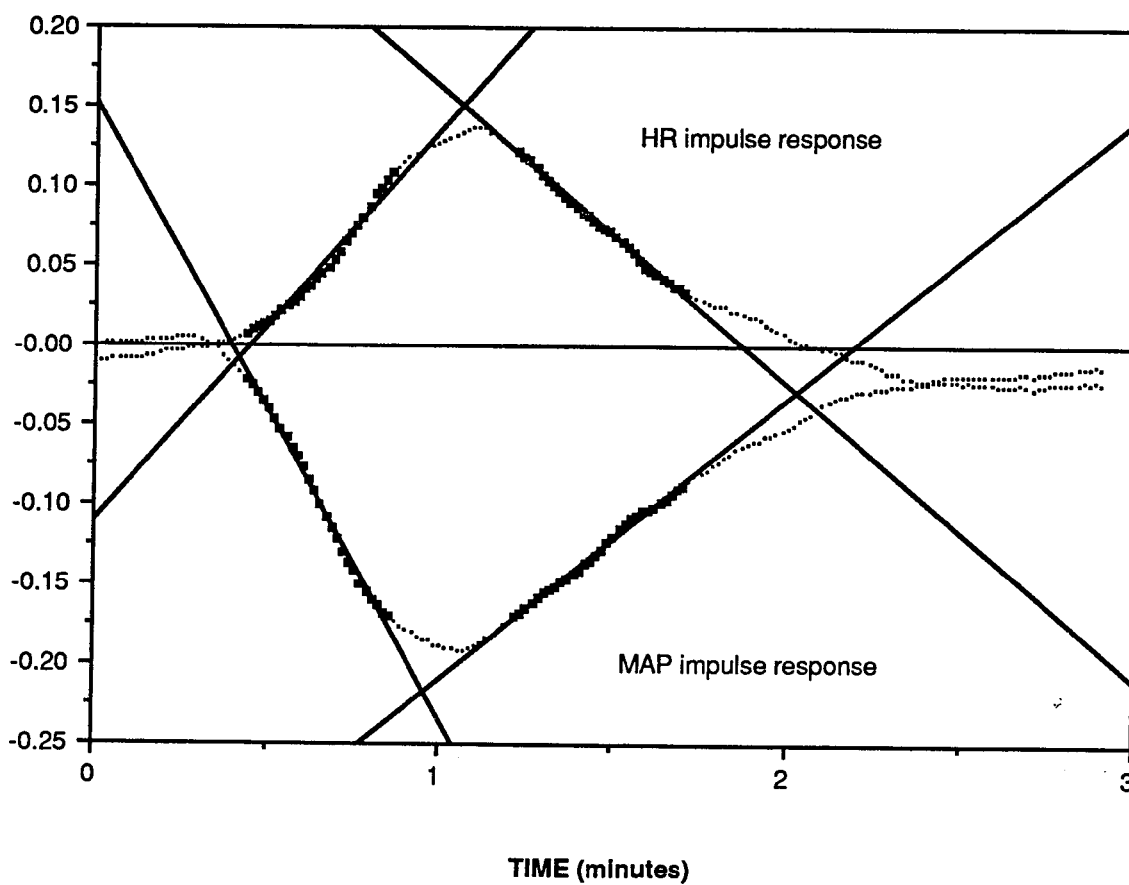


Figure 4-14. Sample computation of response time for baroreceptor heart rate response. Dark data points are those used in linear regression analysis (solid line) to determine x-intercept.

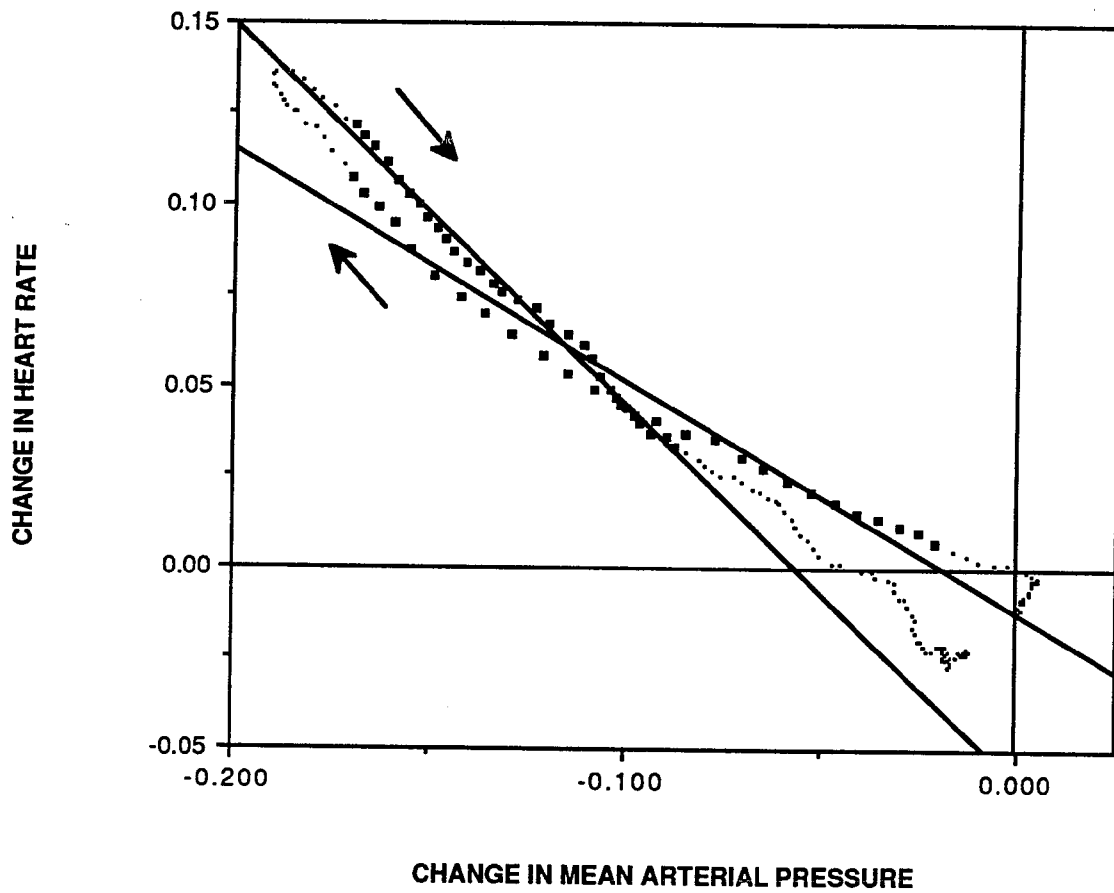


Figure 4-15. Sample computation of baroreceptor heart rate response gain. Dark data points are those used in linear regression analysis (solid lines) to determine activation and deactivation gains.

Table 4-5. Baroreceptor reflex control of heart rate analyzed using impulse response estimates. Data were derived from three types of impulse response estimates: A-crosscorrelation estimate, B-filtered crosscorrelation estimate, C-filtered best approximate estimate.

Dog:	1	2	3	4	5	6
Activation Response Time (minutes)						
A	-.0282	-.1313	-.0969	.0575	-.0082	-.0502
B	-.1175	-.2898	-.2312	-.0120	-.0175	-.0636
C	.1350	-.3518	-.1941	.0154	-.0284	-.0597
Deactivation Response Time (minutes)						
A	.5329	1.8454	.2351	-.2509	.4757	.3769
B	.3487	1.8511	.2384	-.5606	.8403	.2780
C	.2407	1.3824	.1434	-.4507	.6287	.2398
Activation Gain (bpm·mm Hg <sup>-1</sup> )						
A	-.8529	-.1831	-.7208	-.3066	-.5176	-.6285
B	-1.1198	-.0691	-1.1751	-.4186	-.5540	-.6995
C	-.6872	-.3691	-1.0771	-.3604	-.5795	-.6779
Deactivation Gain (bpm·mm Hg <sup>-1</sup> )						
A	-1.9757	-.0878	-1.9400	-.3676	-.9247	-1.0364
B	-1.4357	-.5246	-1.4665	-.2996	-1.0852	-.8765
C	-1.3301	-.4705	-1.4373	-.3082	-1.0230	-.8837

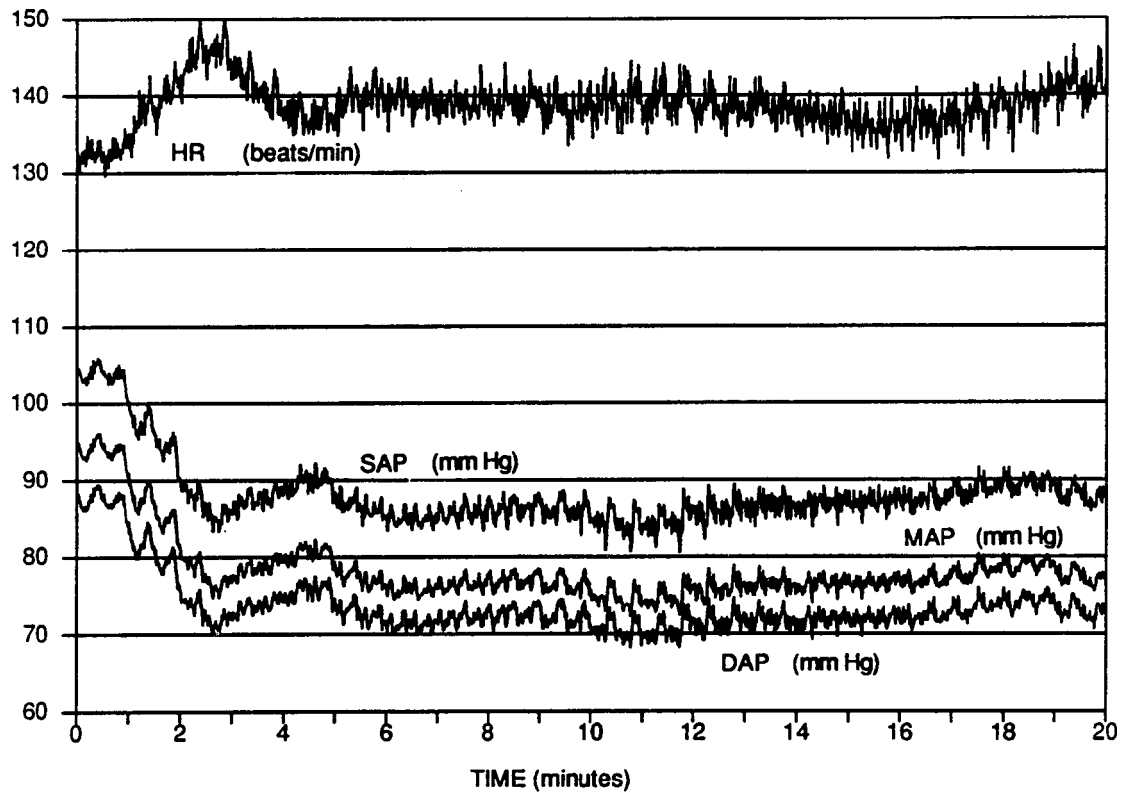


Figure 4-16. Simulation of closed-loop nitroprusside infusion: arterial pressure and heart rate response. Setpoint for mean arterial pressure (controlled variable) was 75 mm Hg.

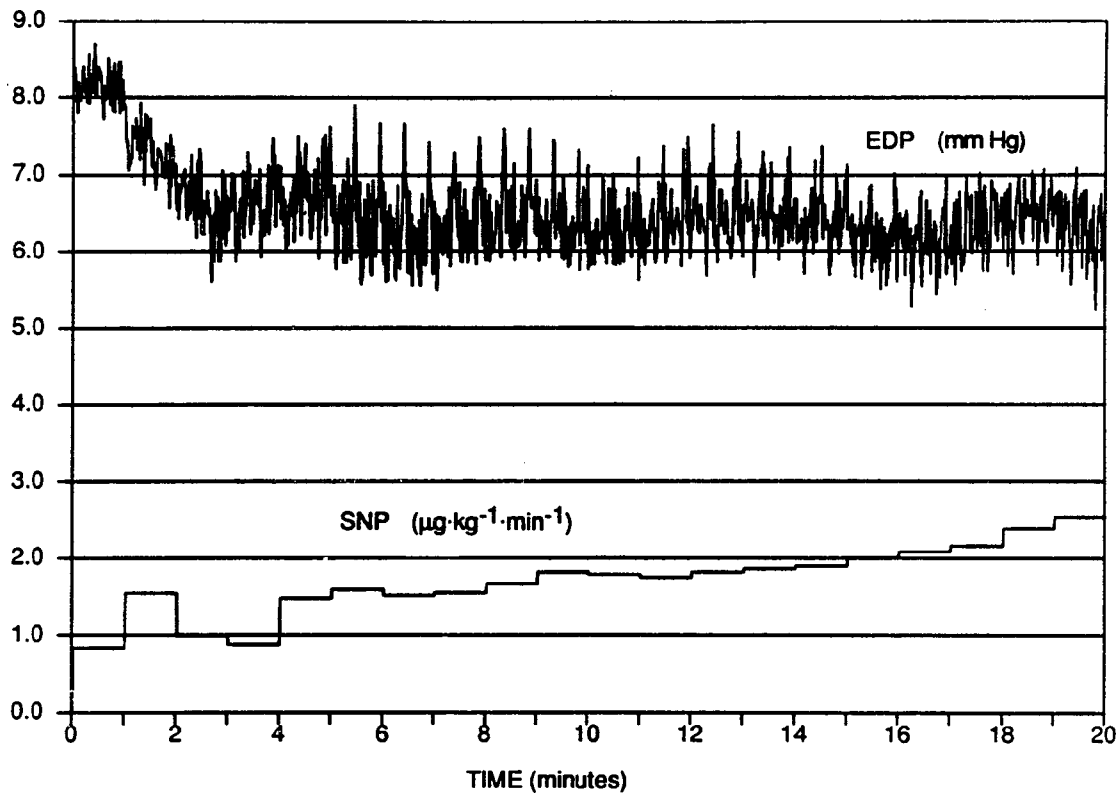


Figure 4-17. Simulation of closed-loop nitroprusside infusion: nitroprusside dose and LV end-diastolic pressure response. Lower tracing: nitroprusside (SNP) infusion rates specified by the control algorithm to achieve the setpoint mean arterial pressure.

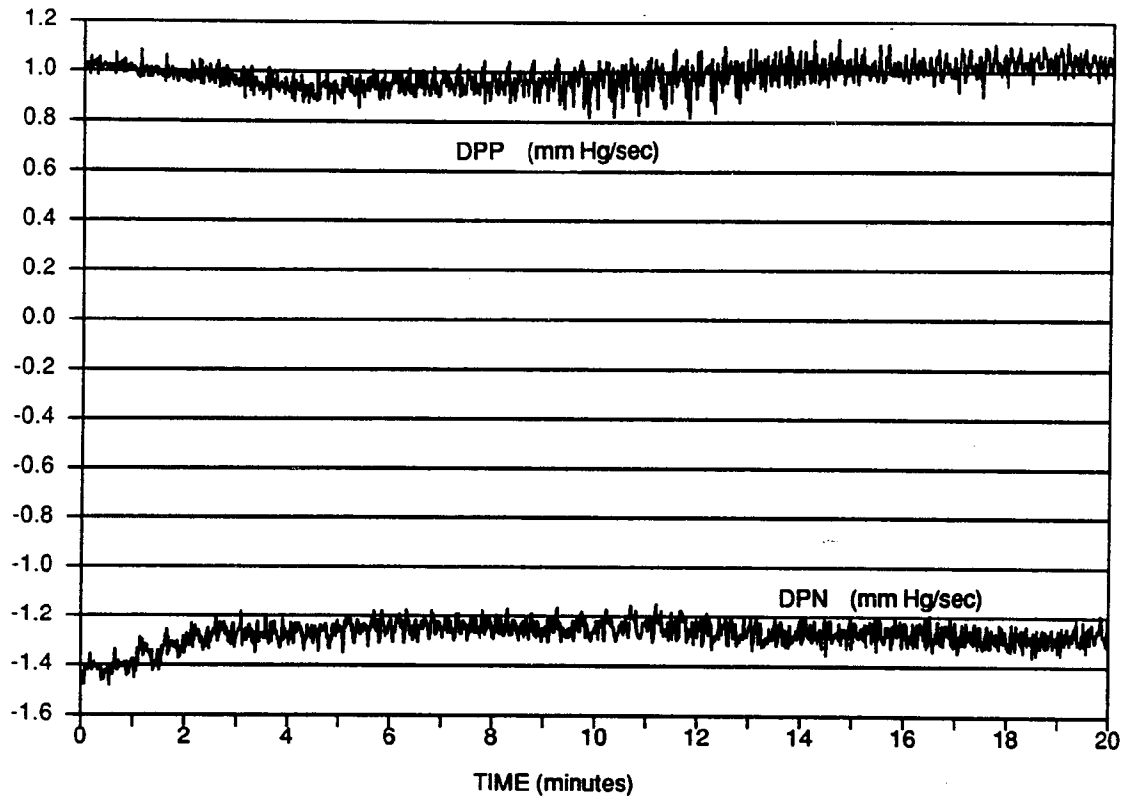


Figure 4-18. Simulation of closed-loop nitroprusside infusion: positive and negative LV  $dP/dt$  response.

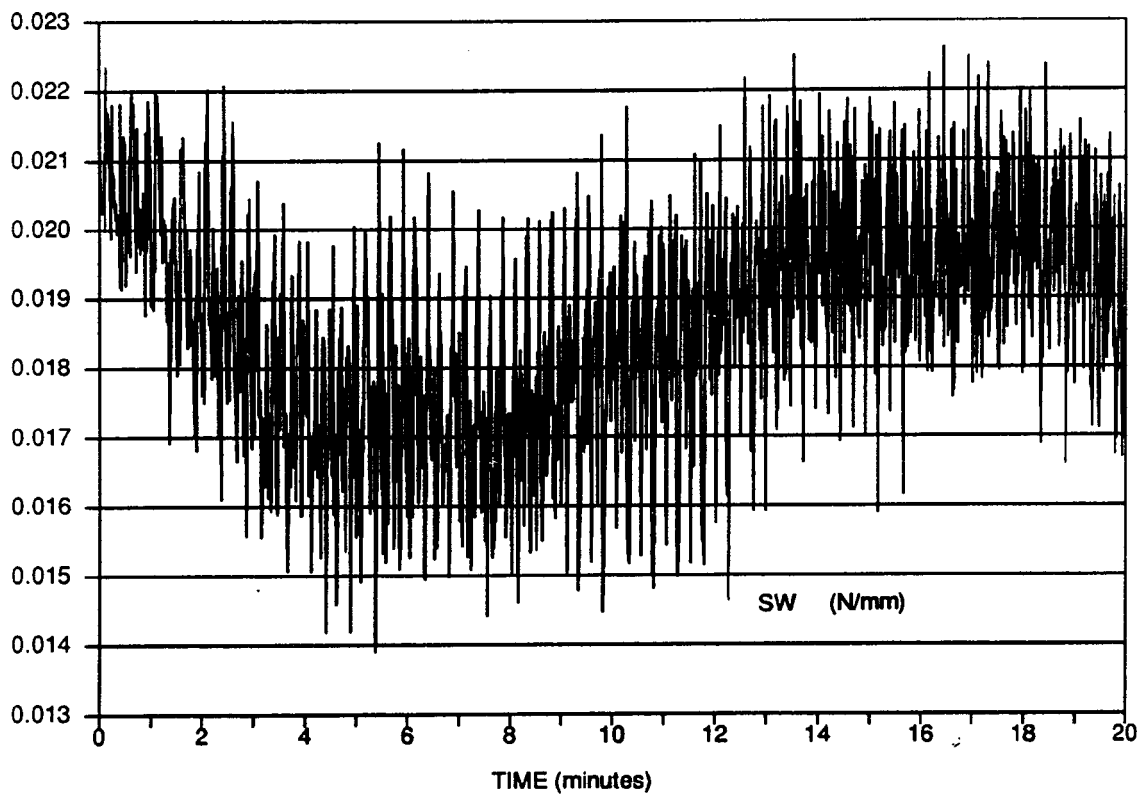


Figure 4-19. Simulation of closed-loop nitroprusside infusion: stroke work response.

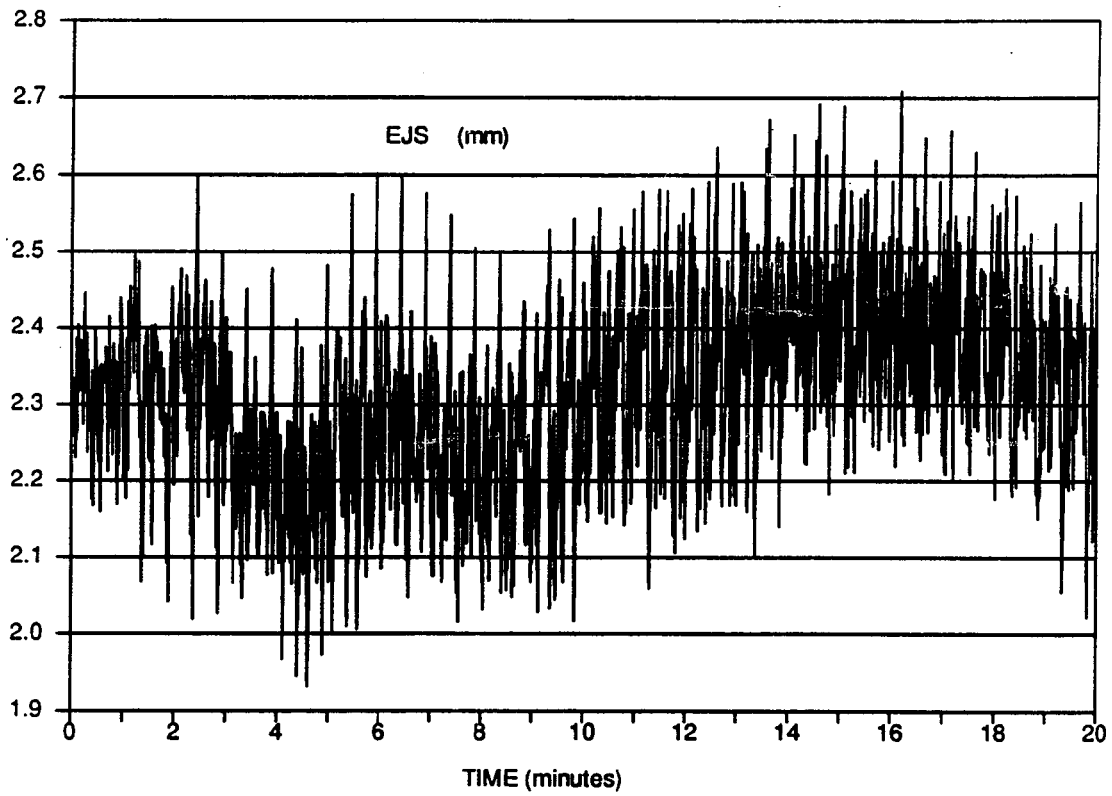


Figure 4-20. Simulation of closed-loop nitroprusside infusion: ejection shortening response

algorithm to maintain the mean arterial pressure setpoint of 75 mm Hg ranged from about 1.0 to 3.5  $\mu\text{g}\cdot\text{kg}^{-1}\cdot\text{min}^{-1}$  and showed a marked upward trend as the simulation progressed. Heart rate during the simulated hypotension settled at a level about 8 bpm above its baseline value following a transiently higher value. End-diastolic LV pressure fell by about 2 mm Hg during the nitroprusside infusion. Peak positive  $dP/dt$  showed little if any change, but peak negative  $dP/dt$  rose to a level substantially above baseline. Stroke work fell initially, then progressed back toward its baseline value as the simulation continued. The ejection shortening data suggested a small initial depression followed by a transient rise above baseline.

## CHAPTER 5

### DISCUSSION

The sequence resulting from crosscorrelating the sampled input and output of a continuous system in PRB testing is a discrete approximation to the continuous impulse response function of the system. This is readily appreciated by rewriting equation (2-3-7) as the following set of simultaneous linear equations:

$$\begin{aligned}
 \phi_{xy}(0) &= \phi_{xx}(0)h(0) + \phi_{xx}(1)h(1) + \cdots + \phi_{xx}(N-1)h(N-1) \\
 \phi_{xy}(1) &= \phi_{xx}(N-1)h(0) + \phi_{xx}(0)h(1) + \cdots + \phi_{xx}(N-2)h(N-1) \\
 &\vdots \\
 &\vdots \\
 \phi_{xy}(N-1) &= \phi_{xx}(1)h(0) + \phi_{xx}(2)h(1) + \cdots + \phi_{xx}(0)h(N-1)
 \end{aligned}
 \tag{5-1}$$

Invoking the approximation that  $\phi_{xx}(i)=0$  for  $i \neq 0$ , as is done in conventional PRB testing, reduces equations (5-1) to

$$\begin{aligned}
 \phi_{xy}(0) &= \phi_{xx}(0)h(0) \\
 \phi_{xy}(1) &= \phi_{xx}(0)h(1) \\
 &\vdots \\
 &\vdots \\
 \phi_{xy}(N-1) &= \phi_{xx}(0)h(N-1)
 \end{aligned}
 \tag{5-2}$$

This is a recapitulation of equation (2-3-9), demonstrating that sampling-dependent parameters (e.g.,  $s$ ) do not explicitly distort the crosscorrelation as an estimate of the sampled impulse response function  $h(t)$ , since  $\phi_{xx}(0)$  is not influenced by sampling. Indeed, the greater the number of samples taken per state of the PRB input, the greater will be  $N$ , and  $\phi_{xx}(n)$  will become ever more impulsive in nature. Of course, the practical consequence of increased sampling is increased temporal resolution of the impulse response estimate. The reality remains, however, that the off-diagonal elements of  $\phi_{xx}$ , particularly those elements representing the triangular portion<sup>1</sup> of  $\phi_{xx}(n)$ , are not equal to zero, and therefore equations (5-2) are only an approximation regardless of the size of  $N$ .

Computation of the best approximate impulse response estimate is equivalent to finding the least-squares solution to the set of  $N$  simultaneous linear equations (5-1), independent of any assumptions about the form of  $\phi_{xx}(n)$ . In so doing, the best approximate, again in the least squares sense, discrete deconvolution of  $h(n)$  and  $\phi_{xx}(n)$  (see equation 2-3-6) is determined, and this, it turns out, is the best approximate impulse response estimate. Techniques for discrete deconvolution have been described [VA-75, NI-76], but are often discounted because of their susceptibility to noise in the data [IN-84]. Hunt [HU-71]

---

<sup>1</sup>As the number of samples taken per state of the PRB signal increases, so will the width (or number of elements in) the triangular portion of  $\phi_{xx}(n)$ .

developed a technique for solving convolution-type integral equations using a matrix approach, and though he did give an extensive analysis of the statistical properties of the solution, he considered only a limited partition of the circulant matrix; this resulted in a coefficient matrix with distinct non-zero eigenvalues but also in a solution much less powerful than the best approximate solution derived in this report.

The relevance of the capability to compute the best approximate impulse response estimate depends upon the purpose for which an estimate of the continuous system's impulse response function is desired. If the intention is to use curve-fitting or other procedures to develop from the discrete impulse response estimate a low-order continuous-time mathematical model (e.g., transfer function) of the system [DA-70, SL-80, GI-85], then the non-normalized crosscorrelation sequence is in general an adequate approximation to the impulse response function. The amplitude of this sequence is inherently correct and is appropriately labeled in units of (system output units) · (PRB input units)<sup>-1</sup>. It is curious to note that in papers presenting crosscorrelation estimates derived from PRB testing it has been common to use a dimensionless [GO-74, SH-77, 80] or ambiguous [GI-85, LI-82, UR-86] scale for the ordinate. In this regard it must be acknowledged that of the impulse response estimates shown in Chapter 4, only the amplitude of the sequence in figure 4-2 (typical non-

normalized crosscorrelation estimate) is labeled correctly as an approximation to the continuous-time impulse response. The amplitudes of all other impulse response estimates given in figures in Chapter 4 are correct in that they give the proper result when used in numerical convolution, but to have the appropriate gain must be multiplied by 29 (=s) if they are to be viewed as discrete approximations to the continuous-time impulse response functions.

If one is interested in using numerical convolution with the discrete impulse response estimate derived from sampled PRB testing to simulate the behavior of the system, then the effects of sampling in the discrete mathematics must be taken into consideration. The simplest way to do this is to divide the crosscorrelation estimate of the impulse response sequence by the number of samples taken per state of the PRB input signal (see Section 2.2.5). As demonstrated in Chapter 4 (e.g., figure 4-9), this normalized crosscorrelation impulse response estimate is a filtered but accurate model of the system. Alternatively, the best approximate impulse response can be computed, which gives an estimate of the system with the fullest possible spectral resolution.

The conclusive validation of an impulse response model is its response to white-noise [MA-78]. Using the PRB sequence as an approximation to white-noise, the best approximate impulse response estimate was shown in Chapter 4 to model the system (hemodynamic responses to nitroprusside)

with amazing fidelity for all of the eleven variables studied. The best approximate impulse response estimate seems to be a very powerful enhancement to PRB testing, primarily because it models both the mean dynamic response and any linearly additive noise. It can be spectrally filtered to provide an impulse response model of any order appropriate for a particular application.

Sheppard [SH-76] pioneered pharmacodynamic identification by PRB testing in intact animals and patients. Sheppard has described mean arterial and left atrial pressure and aortic flow impulse responses to sodium nitroprusside [SH-76, 77] and the aortic flow, femoral flow, coronary flow, mean arterial and left atrial pressures, and heart rate impulse responses to dopamine and epinephrine. Based on Sheppard's successful application of PRB testing with nitroprusside in dogs, this was the model chosen for experimental verification of the theory presented in this paper.

The lack of significant drift (y-intercept and slope in table 4-1) in the hemodynamic parameters measured during the course of the studies and the high degree of correlation between individual and mean impulse response curves (table 4-2) document the stability and quality of the canine preparation used in the present PRB testing experiments. The extremely small mean-square errors (table 4-4) for the best approximate impulse response estimate models attests to the power of this identification technique and to the highly

linear behavior of the system (hemodynamic response to nitroprusside) investigated.

Briefly, the mean impulse response curves (figures 4-4 through 4-7) can be interpreted as follows: Sodium nitroprusside causes relaxation of both arteriolar resistance beds and venous capacitance beds [BL-80]. As a result, not only is there a decrease in systemic vascular resistance but also an increase in peripheral venous capacitance. The former of these effects explains the decrease in arterial pressure and corresponding drop in mean LV ejection pressure, and the later effect explains the fall in preload (end-diastolic LV diameter and pressure). The magnitude of the systolic arterial pressure change was less than that of the diastolic and mean pressures, corroborating the common clinical observation that nitroprusside is less effective in the treatment of systolic hypertension than in diastolic hypertension. The inverse relationship between arterial pressure and heart rate is presumed to be due to the baroreceptor reflex. The rise in peak negative LV  $dP/dt$  is consistent with the known inverse relationship [WI-74] between this parameter and mean arterial blood pressure. The rise in ejection shortening concurrent with falling preload and afterload probably reflects a real, but physiologically insignificant, increase in myocardial contractility due to the liberation of norepinephrine and vagal withdrawal resulting from dysinhibition of the vasomotor center by the baroreflex. Although the striking

similarity between the time course of the ejection shortening and heart rate impulse response curves strongly suggests an autonomic basis for this increase in ejection shortening, it might have been the result of ventricular unloading due to vasodilation by nitroprusside. The lack of distinctive characteristics in the impulse response curves for stroke work and peak positive  $dP/dt$  probably reflects the complex interdependence of these parameters on preload, afterload, and reflex effects, all of which were being dynamically altered during the response to vasodilation. That the response of some of these complex indices of ventricular performance might be somewhat nonlinear is suggested by the higher mean-square errors (table 4-4) for these parameters than for mean arterial pressure, for example.

As an example of direct use of the derived impulse response estimates to provide physiological information, the response time and closed-loop gain of the baroreceptor heart rate control system were determined from the heart rate and mean arterial pressure impulse response estimates. The known hysteresis in the baroreceptor reflex was apparent in this study and is probably indicative of a time-rate-of-pressure-change component in the integrated baroreceptor response. Though the small sample sizes and the lack of control data verified by another measurement technique preclude statistical confirmation, appropriately filtered best approximate impulse response estimates would presumably

provide the most accurate data in this type of application. Chen et al. [CH-82] used bolus injections of nitroprusside to perform a similar analysis, but their technique raises the issue of large amplitude nonlinearities; the advantage of PRB testing is clear in this regard. If the system can be considered to be linear over the operating range tested, it is completely described by its impulse response, and this type of analysis deserves further investigation.

Implicitly or explicitly, the motivation behind PRB testing is to develop a model of the system under investigation. Willems [WI-86] has recently defined the most powerful unfalsified model as that model which explains a given set of observations and as little else as possible. To the extent that it is the best approximate deconvolution of the observations (discrete input/output samples of the system response to the PRB signal), the best approximate impulse response estimate is the most powerful, to use Willems' terminology, model obtainable from PRB testing in that it "explains" the response of the system to the PRB input. This was attested to in the present study by the trivial difference (mean-square error) between the original data sequences and the sequences generated by convolution of the best approximate impulse response estimate with its respective PRB sequence. However, a model that explains only the system response to the perturbations used to derive it is of little practical relevance. Indeed, the purpose of PRB testing is to identify a model (impulse response

estimate) capable of predicting the system output for any appropriate input. The best approximate impulse response estimate facilitates realistic and accurate numerical simulations of practical relevance, as was demonstrated in this report for the closed-loop infusion of nitroprusside; such simulations might be useful in control system design, for example. It is proposed that the greatest utility for the best approximate impulse response sequence is in numerical simulations where realistic modeling of the dynamic and background components is desired but where separate consideration of these elements is not required. The best approximate impulse response estimation algorithm should eventually be of interest in many identification, adaptive signal processing, and adaptive control applications.

Willems [WI-86] goes on to state:

...in most applications the lack of fit between data and model is not in the first place due to randomness or measurement noise but to the fact that one consciously uses a model whose structure is unable to capture the complexity of the phenomenon which one is observing. . . . [B]efore setting up algorithms for obtaining . . . approximate models it seems reasonable that one should be able to produce algorithms for obtaining exact models.

In PRB testing, the best approximate impulse response estimate derived in this report is as close to an exact model as it is possible to obtain. Through selective filtering of the best approximate solution it should be possible to acquire an approximate model of any desired

resolution or to separate the dynamic and background components of the system response. This raises the prospect of reversing the traditional approach to system modeling where estimates of background activity are added piecemeal to an approximate model of the dynamic response; using the best approximate impulse response estimate it may be possible to derive from the single "exact" solution each of its individual components and in so doing to systematically formulate a complete and rich model.

Finally, it is remarkable to note that calculation of the best approximate solution (equation 2-4-5) is an algorithm of general applicability, not restricted to PRB testing. Other than to assume that the input sequence was periodic and that its autocorrelation matrix was singular, at no point in the derivation of the best approximate solution was any assumption made regarding the form of the sampled input sequence. Thus, equation 2-4-5 can always be used to find the unique least squares solution or the solution of minimum norm of the system of equations (5-1). When  $x(t)$  is well-behaved and of bandwidth greater than that of the system, e.g., a PRB test signal, the solution  $h(n)$  will be the best approximate impulse response estimate.

It has been suggested [WA-86] that the principal contribution of an article is either new observations ("results") or development of a new way of looking at the world. Although novel data describing the pharmacodynamics of sodium nitroprusside have been obligatorily obtained to

provide experimental verification of theory, possibly the greater contribution of this work would be to stimulate the development of innovative and powerful approaches to system modeling and simulation as the simple algorithm derived here to find the best approximate impulse response estimate is refined and exploited.

#### LIST OF REFERENCES

- [BA-75] H. A. Barker and R. W. Davy, "System identification using pseudorandom signals and the discrete Fourier transform," Proc. IEE, vol. 122, pp. 305-311, 1975.
- [BE-79] H. A. Beagley, B. McA. Sayers, A. J. Ross, "Fully objective ERA by phase spectral analysis," Acta Otolaryngol., vol. 87, pp. 270-278, 1979.
- [BL-80] T. F. Blaschke and K. L. Melmon, "Antihypertensive agents and the drug therapy of hypertension," in The Pharmacological Basis of Therapeutics, A. G. Gilman, L. S. Goodman, A. Gilman, Eds. New York: Macmillan, 1980, pp. 805-806.
- [BU-77] C. R. Burrows and R. Stanway, "Identification of journal bearing characteristics," J. Dynamic Sys. Meas. Cont., vol. 99, pp. 167-173, 1977.
- [BU-81] C. R. Burrows, R. Sayed-Esfahani, R. Stanway, "A comparison of multifrequency techniques for measuring the dynamics of squeeze-film bearings," J. Lubrication Tech., vol. 103, pp. 137-143, 1981.
- [CH-82] R. Y. Z. Chen, F. Fan, G. B. Schuessler, S. Chien, "Baroreflex control of heart rate in humans during nitroprusside-induced hypotension," Am. J. Physiol., vol. 243, pp. R18-R24, 1982.
- [CL-70a] D. W. Clarke and P. A. N. Briggs, "Errors in weighting sequence estimation I. A matrix formulation," Int. J. Control, vol 11, pp. 49-56, 1970.
- [CL-70b] D. W. Clarke and P. A. N. Briggs, "Errors in weighting sequence estimation II. The effects of autocorrelated noise," Int. J. Control, vol 11, pp. 57-65, 1970.
- [DA-70] W. D. T. Davies, System Identification for Self-Adaptive Control. London: John Wiley and Sons, 1970, pp. 25-88.

- [DA-79] P. J. Davis, Circulant Matrices. New York: John Wiley and Sons, 1979, pp. 16-91.
- [EA-64] M. F. Easterling, "Modulation by pseudo-random sequences," in Digital Communications with Space Applications, S. W. Golomb, Ed. Englewood Cliffs, NJ: Prentice-Hall, 1964, p.76.
- [EY-74] P. Eykhoff, System Identification. London: John Wiley and Sons, 1974, 555 pp.
- [GI-85] M. H. Giard, F. Perrin, O. Bertrand, D. Robert, J. Pernier, "An algorithm for automatic control of O<sub>2</sub> and CO<sub>2</sub> in artificial ventilation," *IEEE Trans. Biomed. Eng.*, vol. BME-32, pp. 658-667.
- [GL-85] D. D. Glower, J. A. Spratt, N. D. Snow, J. S. Kabas, J. W. Davis, C. O. Olsen, G. S. Tyson, D. C. Sabiston, J.S. Rankin, "Linearity of the Frank-Starling relationship in the intact heart: the concept of preload recruitable stroke work," *Circulation*, vol. 71, pp. 994-1009, 1985.
- [GO-74] K. R. Godfrey and D. J. Moore, "Identification of processes having direction-dependent responses, with gas-turbine engine applications," *Automatica*, vol. 10, pp. 469-481, 1974.
- [GO-80] K. R. Godfrey, "Correlation methods," *Automatica*, vol. 16, pp. 527-534, 1980.
- [GO-82] S. W. Golomb, Shift Register Sequences. Laguna Park, CA: Aegean Park Press, 1982, 247 pp.
- [GO-85] R. J. Gorczynski, "Basic pharmacology of esmolol," *Am. J. Cardiol.*, vol. 56, pp. 3F-13F, 1985.
- [GR-83] F. A. Graybill, Matrices with Applications in Statistics. Belmont, CA: Wadsworth, 1983, pp. 149-289.
- [GU-75] I. Gufstavsson, "Survey of applications of identification in chemical and physical processes," *Automatica*, vol. 11, pp. 3-24, 1975.
- [HU-71] B. R. Hunt, "Biased estimation for nonparametric identification of linear systems," *Math. Biosci.*, vol. 10, pp. 215-237, 1971.
- [IN-84] D. Ingram and R. Bloch, Mathematical Methods in Medicine Part 1 Statistical and Analytical Techniques. Chichester, England: John Wiley and Sons, 1984, pp. 377-380.

- [IS-80] R. Isermann, "Practical aspects of process identification," *Automatica*, vol. 16, pp. 575-587, 1980.
- [LA-70] J. D. Lamb, "System frequency response using p-n binary waveforms," *IEEE Trans. Auto. Control*, vol. AC-15, pp. 478-480, 1970.
- [LE-82] K. M. Letherman, C. J. Palin, P. M. Park, "The measurement of dynamic thermal response in rooms using pseudo-random binary sequences," *Build. Environ.*, vol. 17, pp. 11-16, 1982.
- [LI-81] D. A. Linkens, S. J. Rimmer, A. J. Asbury, B. H. Brown, "Identification of the model in the control of neuromuscular blockade using PRBS testing," (Abstract) *Br. J. Anaesth.*, vol. 53, p. 666P, 1981.
- [LI-82] D. A. Linkens, A. J. Asbury, S. J. Rimmer, M. Menad, "Identification and control of muscle-relaxant anaesthesia," *IEE Proc.*, vol. 129, pp. 136-141, 1982.
- [MA-78] P. Z. Marmarelis and V. Z. Marmarelis, Analysis of Physiological Signals. New York: Plenum, 1978, 487 pp.
- [MO-73] D. M. Monro, "Algorithm: fast fourier transform," London: Imperial College of Science and Technology, Application Report No. 5, 19 pp., 1973.
- [NI-76] A. J. Niemi, "On discrete deconvolution," *Med. Biol. Eng.*, vol. 14, pp. 582-584, 1976.
- [OL-84] C. O. Olsen, S. J. Abert, D. D. Glower, J. A. Spratt, G. S. Tyson, J. W. Davis, J. S. Rankin, "A hermetically sealed cardiac dimension transducer for long-term animal implantation," *Am. J. Physiol.*, vol. 247, pp. H857-H860, 1984.
- [OP-75] A. V. Oppenheim and R. W. Schaffer, Digital Signal Processing. Englewood Cliffs, NJ: Prentice-Hall, 1975, 575 pp.
- [PE-55] R. Penrose, "On best approximate solutions of linear matrix equations," *Proc. Camb. Phil. Soc.*, vol. 52, pp. 17-19, 1955.
- [PO-74a] J. Ponte and M. J. Purves, "Receptor dynamics using correlation techniques," *Med. Biol. Eng.*, vol. 12, pp. 792-799, 1974.

- [PO-74b] J. Ponte and M. J. Purves, "Measurement of the frequency response of carotid sinus baroreceptors in the cat," *Med. Biol. Eng.*, vol. 12, pp. 800-802, 1974.
- [PO-77] D. Poussart and U. S. Ganguly, "Rapid measurement of system kinetics - an instrument for real-time transfer function analysis," *Proc. IEEE*, vol. 65, pp. 741-747, 1977.
- [PY-82] P. B. Pynsent and R. Hanka, "A simple program for a phaseless recursive digital filter," *J. Biomed. Eng.*, vol. 4, pp. 252-254, 1982.
- [QU-86] C. Y. Quon and R. J. Gorczynski, "Pharmacodynamics and onset of action of esmolol in anesthetized dogs," *J. Pharmacol. Exp. Ther.*, vol. 237, pp. 912-918, 1986.
- [RE-78] J. G. Reves, L. C. Sheppard, R. Wallach, W. A. Lell, "Therapeutic uses of sodium nitroprusside and an automated method of administration," *Int. Anesth. Clinics*, vol. 16, pp. 51-88, 1978.
- [RU-73] H. J. Rubenstein, T. Kenner, K. Ono, "Pseudorandom testing technique for the characterization of local hemodynamic control," *Pflugers Arch.*, vol. 343, pp. 309-316, 1973.
- [SH-76] L. C. Sheppard, "Correlation analysis of arterial blood pressure responses to vasoactive drugs with particular reference to clinical surveillance of the post surgical patient," Ph.D. dissertation, University of London, 1976.
- [SH-77] L. C. Sheppard and B. McA. Sayers, "Dynamic analysis of the blood pressure response to hypotensive agents, studied in postoperative cardiac surgical patients," *Comp. Biomed. Res.*, vol. 10, pp. 237-246, 1977.
- [SH-80] L. C. Sheppard, B. McA. Sayers, W. F. Holdefer, H. C. CoGhlan, "Assessment of the dynamics of cardiac responses to positive inotropic agents," in Cardiac Dynamics, J. Baan, A. C. Arntzenius, E. L. Yellin, Eds. The Hague: Martinus Nijhoff, 1980, pp. 395-404.

- [SH-82] L. C. Sheppard, W. F. Holdefer, N. T. Kouchoukos, J. W. Kirklin, "Analysis of the multiple effects of vasoactive and positive inotropic agents on cardiovascular system variables," in Cardiovascular System Dynamics: Models and Measurements, T. Kenner, R. Busse, H. Hinghofer-Szalkay, Eds. New York: Plenum, 1982, pp. 647-655.
- [SL-80] J. B. Slate, "Model-based design of a controller for infusing sodium nitroprusside during post surgical hypertension," Ph.D. dissertation, University of Wisconsin-Madison, p. 36, 1980.
- [SU-74] H. Suga and K Sagawa, "Assessment of absolute volume from diameter of the intact canine left ventricular cavity," J. Appl. Physiol., vol. 36, pp. 496-499, 1974.
- [TO-73] M. Toll, "Systems analysis of inotropic interventions in isolated heart muscle," Ph.D. dissertation, University of London, 1973.
- [UR-86] L. B. Uribe and J. A. Gallegos, "Identification of a binary distillation column," Int. J. Systems Sci., vol. 17, pp. 295-304.
- [VA-75] M. E. Valentinuzzi and E. M. M. Volachec, "Discrete deconvolution," Med. Biol. Eng., vol. 13, pp. 123-125, 1975.
- [WA-86] B. E. Waud and D. R. Waud, "Dose-response curves and pharmacokinetics," Anesthesiology, vol. 65, pp. 355-358, 1986.
- [WI-74] M. L. Weisfeldt, H. E. Scully, J. Frederiksen, J.J. Rubenstein, G. M. Pohost, E. Beierholm, A. G. Bello, W. M. Daggett, "Hemodynamic determinants of maximum negative  $dp/dt$  and periods of diastole," Am. J. Physiol., vol. 227, pp. 613-621, 1974.
- [WI-86] J. C. Willems, "From time series to linear system - Part II. Exact modelling," Automatica, vol. 22, pp. 675-694, 1986.

## APPENDIX A

### CIRCULANT INVERSION

The following Fortran listing provides the salient features of the software program written to compute the generalized inverse of the circulant autocorrelation matrix (see Section 2-4). SETWT and CHRFT were double precision implementations of the subroutines of the same name by Monro [MO-73].

```
C
C   PROGRAM CIRCINV.FOR
C
C
C   REAL*8 WR(4096),WI(4096),RL(4096),IM(4096),SMALL
C   .
C   .
C   .
C   READ FILE CONTAINING FIRST ROW OF CIRCULANT MATRIX FOR
C   WHICH THE INVERSE IS TO BE COMPUTED; MAY CONTAIN UP TO
C   2048 ELEMENTS. THE SEQUENCE OF LENGTH N IS STORED IN
C   ARRAY RL.
C
C   .
C   .
C   .
C   SET UP FOURIER TRANSFORMED CHIRP FUNCTION FOR USE BY
C   SUBROUTINE CHRFT
C
C   CALL SETWT(WR,WI,N,4096)
C
C   CALCULATE THE EIGENVALUES OF THE CIRCULANT MATRIX BY
C   FINDING THE INVERSE DFT OF THE FIRST ROW OF THE
C   CIRCULANT MATRIX. CHRFT COMPUTES THE DISCRETE FOURIER
C   TRANSFORM OF A DATA SEQUENCE WITH REAL PART RL AND
C   IMAGINARY PART IM BY THE CHIRP-Z TRANSFORM.
C
C   CALL CHRFT(RL,IM,WR,WI,-N,4096)
```

```
C
C   PERFORM RECIPROCATION OF THE EIGENVALUES.  IM SHOULD BE
C   ZERO, SINCE THE AUTOCORRELATION IS AN EVEN FUNCTION, AS
C   WILL BE THE SEQUENCE OF EIGENVALUES.
C
SMALL=DBLE(1.E-11)
DO 100 I=1,N
    IF(DABS(RL(I)).GT.SMALL) THEN
        RL(I)=DBLE(1.)/RL(I)
    ELSE
        RL(I)=DBLE(0.)
    ENDIF
    IM(I)=DBLE(0.)
100 CONTINUE
C
C   COMPLETE CALCULATION OF THE GENERALIZED CIRCULANT
C   INVERSE BY COMPUTING FORWARD DFT OF THE RECIPROCAL
C   EIGENVALUES
C
CALL CHRFT(RL,IM,WR,WI,N,4096)
C
C   STORE RL WHICH, BECAUSE THE GENERALIZED INVERSE IS ALSO
C   A CIRCULANT, DEFINES THE ENTIRE INVERSE MATRIX.
C
.
.
.
END
```

## APPENDIX B

### SIMULATION OF CLOSED-LOOP NITROPRUSSIDE

The following Fortran listing provides the salient features of the software program written to simulate closed-loop infusion of sodium nitroprusside. See Section 3.2.

```
C
C Program SNPBPSIM.FOR
C
C     REAL*8 GNEW(0:2000),CON(0:2000),A(0:2000),SUM
C     REAL*8 TERM,DELTAI,K,BP,E,E1,INFRATE
C     INTEGER PAVG,SETPT,CNT,MAP0,P,P1,P2,P3,P4,P5
C
C     SET THE VARIABLE MAP0 EQUAL TO THE BASELINE (dc)
C     BLOOD PRESSURE
C
C     SET THE VARIABLE SETPT EQUAL TO THE DESIRED SETPOINT
C     MEAN ARTERIAL BLOOD PRESSURE
C
C     READ THE FILE CONTAINING THE TIME-SHIFTED BEST
C     APPROXIMATE IMPULSE RESPONSE SEQUENCE FOR MEAN ARTERIAL
C     PRESSURE AND STORE IN ARRAY GNEW(1827)
C
C     INFUSION RATES ARE STORED IN ARRAY A
C
C     SET INITIAL INFUSION RATE TO 0
C     INFRATE=DBLE(0.)
C
C     INITIALIZE TIMER TO 0
C     CNT=0
C
C     INITIALIZE ARRAYS
C     DO 510 I=0,1826
C         A(I)=DBLE(0.)
510     CON(I)=DBLE(0.)
C
C     SIMULATE 1827 SECONDS OF DATA
```

```

DO 600 I=0,1826
C      DO NUMERICAL CONVOLUTION TO DETERMINE CURRENT
C      CHANGE IN BLOOD PRESSURE DUE TO DRUG
      DO 520 II=0,I
          LAG=I-II
          CON(I)=CON(I)+GNEW(II)*A(LAG)
520      CONTINUE
C
C      CURRENT BLOOD PRESSURE IS EQUAL TO THE BASELINE
C      PRESSURE PLUS THE CHANGE IN PRESSURE DUE TO THE DRUG
      P=MAP0+INT(CON(I))
C      DETERMINE MEAN ARTERIAL PRESSURE AS THE AVERAGE OF
C      LAST 6 MEASUREMENTS
      PAVG=(P1+P2+P3+P4+P5+P)/6
C      IF 60 SECONDS HAVE PASSED RESET INTERVAL
C      COUNTER AND CONTINUE OTHERWISE GOTO 548
      IF(CNT.EQ.60) THEN
          CNT=0
      ELSE
          GOTO 548
      ENDIF
C      IMPLEMENT SHEPPARD'S CONTROL ALGORITHM
      E=DBLE(SETPT-PAVG)
      IF(PAVG.GE.SETPT+5) K=-1.
      IF((PAVG.GE.SETPT).AND.(PAVG.LT.SETPT+5)) K=-.5
      IF((PAVG.LT.SETPT).AND.(PAVG.GE.SETPT-5)) K=-1.
      IF(PAVG.LT.SETPT-5) K=-2
      TERM=DBLE((.4512*E)+(.4512)*(E-E1))
      DELTAI=K*TERM
      IF(DELTAI.GT.7.) DELTAI=7.
      IF(PAVG.GT.SETPT+5) DELTAI=DELTAI-2.
      IF((PAVG.LT.SETPT-5).AND.(DELTAI.GT.0.)) DELTAI=0.
      INFRATE=INFRATE+DELTAI
      IF(INFRATE.LT.DBLE(0.0)) INFRATE=DBLE(0.)
C
C      CONVERT THE ML/HR INFUSION RATE TO MCG/KG/MIN (200
C      MCG/ML, 20 KG, 60 MIN/HR)
548      A(I+1)=INFRATE*DBLE(.16666)
          E1=E
C      INCREMENT THE COUNTER AND UPDATE THE PRESSURE STORAGE
C      VARIABLES
          CNT=CNT+1
          P1=P2
          P2=P3
          P3=P4
          P4=P5
          P5=P
600      CONTINUE
C
C      ADD THE BASELINE PRESSURE TO EACH ELEMENT IN THE ARRAY
C      (CON) OF DYNAMIC PRESSURE RECORDINGS AND WRITE THE
C      DATA TO A FILE
C
C

```

```
.  
. .  
C  
C SAVE FILE OF INFUSION RATES FOR SUBSEQUENT CONVOLUTION  
C WITH IMPULSE RESPONSES FOR OTHER VARIABLES.  
. .  
END
```

GRADUATE SCHOOL  
UNIVERSITY OF ALABAMA AT BIRMINGHAM  
DISSERTATION APPROVAL FORM

Name of Candidate James Ralph Jacobs

Major Subject Biomedical Engineering

Title of Dissertation Best Approximate Impulse Response Estimate in  
Pseudo-Random Binary Sequence System Identification with Application  
to Sodium Nitroprusside Pharmacodynamics

Dissertation Committee:

Eric C Shopp, Chairman

Martin J McArthur

J. D. Ruggins

John C Bess

Virginia Cooper

Director of Graduate Program

Eric C Shopp

Dean, UAB Graduate School

Anthony Bann

Date February 13, 1987